PHYSICAL REVIEW D VOLUME 4, NUMBER 2 15 JULY 1971

High-Energy Elastic and Inelastic Scattering in φ^3 Theory

Shau-Jin Chang*
Department of Physics, University of Illinois, Urbana, Illinois 61801

and

Tung-Mow Yan†
Laboratory of Nuclear Studies, Cornell University, Ithaca, New York 14850
(Received 16 February 1971)

We study high-energy elastic and inelastic processes in a φ^3 theory based on the following model: For the elastic-scattering amplitude we first sum the leading terms in each order of perturbation of the t-channel straight ladders, plus those obtained by interchange of the Mandelstam variables s and u. We then perform the s-channel iteration with the t-channel ladders as single units. We are only interested in the physical regions in which the incident particles retain their large momenta. This procedure leads to the eikonalization of the t-channel ladders. For the inelastic production amplitude, the dominant contribution comes from diagrams with any number of totally open ladders (i.e., multiperipheral chains) modified by unopen ones. The main results are: (a) The total cross section approaches zero, approaches a constant, or increases as $(\ln s)^2$ according as the coupling constant is smaller than, equal to, or larger than a critical value. (b) Elastic and inelastic differential cross sections are computed, and they have many nice features, as suggested by the absorption model. (c) Nonforward s-channel unitarity is explicitly verified. (d) One-particle and multiparticle spectra, the average multiplicity, the number distribution of the final particles, etc., are obtained. The implications of these results to hadron physics are discussed.

I. INTRODUCTION

Even though quantum field theory may be the only theoretical structure which incorporates all fundamental properties of relativistic invariance, quantum superposition, unitarity, etc., it has not proved to be very successful in the analysis of high-energy scattering in strong interactions, because of the lack of a better alternative to the conventional perturbation expansion. People thus have turned to phenomenological frameworks such as the Regge theory and the absorption model. These theories are based on ideas abstracted from nonrelativistic potential scattering, and are not precisely formulated relativistically. In particular, the production processes and their connection with elastic scattering through unitarity constraints have not been studied in detail, with the possible exception of the multiperipheral model.[1] Some qualitative predictions about inelastic production have been made by the recently proposed parton model[2] and the hypothesis of limiting fragmentation.[3] These models are also semiphenomenological in the sense that many of the abstracted empirical facts are taken as inputs in the formalism. As the recently developed infinite-momentum technique enables one to handle the leading high-energy behavior of a very wide class of Feynman diagrams,[4-9] it is hoped that study of certain field-theory models will at least reveal some general qualitative features concerning the questions mentioned above. Much work along this line has been done by many authors.[6-10] Some nice features of the scattering theory, which previously could only be understood through analogy with nonrelativistic potential scattering, can now be related to the contribution from the sum of certain classes of Feynman amplitudes.

On the basis of their results of high-order calculations of the elastic-scattering amplitude in massive quantum electrodynamics (QED), Cheng and Wu[6] recently made a number of predictions on the elastic-scattering amplitude, on the differential and integrated elastic cross section, and on the total cross section for hadron-hadron scattering at infinite energy. Their central results derive from the fact that the sum of the $(\ln s)^N$ factors in the "tower diagrams" exponentiates to a power of s, and the s-channel iteration of these tower diagrams gives an eikonal form. These logarithmic factors $(\ln s)^N$ have been naturally attributed to a purely longitudinal phase-space effect.[8] The eikonal form emerges from the intuitive expectation that in the infinite-energy c.m. system, because of Lorentz contraction, the colliding particles have almost instantaneous interactions as they pass through each other. Hence, the potential picture should apply. Since the result is essentially kinematic in origin, one may expect that a simple model with φ^3 coupling will also give the same qualitative predictions as QED. Furthermore, the simplicity of the model allows one to draw more physical consequences. The search for a simple model is motivated by the belief that these field-theoretical model calculations have value mainly in extracting physical pictures. The essential physical content, we believe, is best illustrated by the use of the simplest possible mathematics.

Previously, there has been some reservation in pursuing the perturbation calculation in φ^3 theory because, to any finite order of perturbation expansions, the high-order diagrams are always smaller than the Born term by at least a power of s, within powers of $\ln s$. Hence, if one believes in the philosophy of keeping only the leading terms in the perturbation theory, one should only keep the Born term, which is not interesting. However, it is well known that after summing over a selected set of diagrams, such as t-channel ladders, the resultant amplitude may acquire an s dependence which is larger than each of the individual terms. In fact, the sum over t-channel ladders leads to a Regge pole,[11] whose intercept $\alpha(0)$ is a function of the coupling constant g^2. For large g^2, $\alpha(0)$ becomes positive. Consequently, the amplitude due to these ladder exchanges dominates over the Born term. This result demonstrates that accumulation of diminishingly small effects may become important. It also suggests that one could not draw any definite quantitative conclusion from a perturbative leading-term-summation calculation, since it is not possible to establish that terms neglected will not add to a comparable contribution. Thus, one should be careful about how to use perturbation theory as a guide. Although these leading-term summations may not be reliable numerically, the results could still be qualitatively useful. What we primarily search for are the physical mechanisms and pictures associated with certain high-energy characteristics of the scattering amplitudes. A simple example of such an association is that of the $\ln s$ factors with the degrees of freedom in the longitudinal phase space mentioned before. Understanding the underlying mechanisms and physical pictures responsible for the high-energy behavior of the scattering amplitudes is the principal goal of any diagram analysis. This understanding will help us to anticipate what general qualitative features might persist, or in what way they might be modified when the analysis is extended to include a wider class of diagrams and/or to keep more nonleading terms. Hence, one should feed in additional physical requirements to select the set of diagrams, and/or the specific integration regions that one should analyze in order to understand a particular mechanism.

In this paper, we report in some detail predictions on elastic and *inelastic* hadron scattering at very high energies, based on a simple φ^3 model. The main results of this paper were published in a Letter.[12] The set of diagrams that we have studied in this paper is the s-channel iteration of t-channel ladders (see Fig. 1). The legs of the ladders are permuted in all possible ways on the incident-particle lines. We are only interested in the kinematic region in which the incident particles retain their large momenta during the scattering, i.e., the legs of the exchange ladders do not carry any appreciable fraction of the large incident momenta. The s-channel iteration of these ladders in the manner described above gives the standard eikonal form.[6,8,13] A t-channel ladder is the simplest connected exchange which gives rise to an absorptive part in the eikonal function. Hence, it leads to nontrivial production processes. It can be shown that the inclusion of any other connected exchange does not affect our qualitative predictions. Thus we are content with our simple model.

We would like to emphasize here that the main purpose of this paper is *not* to study the validity of the eikonal approximation for the diagrams under consideration by analyzing the leading $(\ln s)^N$ terms in each diagram. Rather, we are extracting that part of the iterated ladder graphs whose asymptotic behavior of the sum possesses a simple physical interpretation. The kinematical region in which the incident particles retain their large momenta does not necessarily pick up the leading terms of each individual diagram. This point was studied

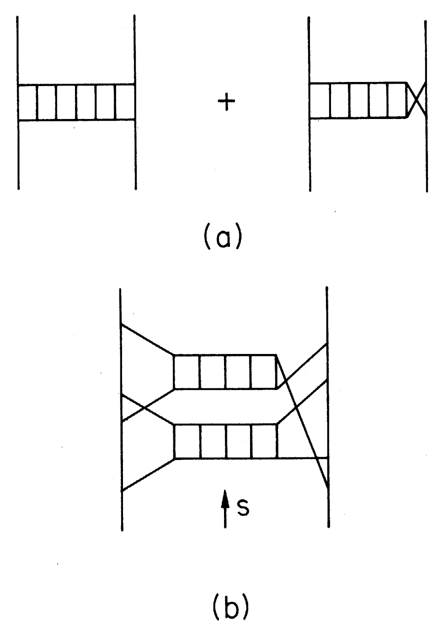

FIG. 1. (a) t-channel ladders. (b) Example of s-channel iteration of the t-channel ladders in (a); permutation among the legs of all ladders is understood.

in a recent paper of Cicuta and Sugar and will be discussed in a note added to this article.

The physical reason for making the above kinematic restriction will be given in Sec. II. Here we merely mention that with this restriction only pionization processes are considered in which the secondary particles have small momenta in comparison with the incident momenta in the c.m. system. As we shall see later, pionization is the dominant mechanism contributing to the total cross sections at very high energies.

We also study the inelastic processes which contribute to the absorptive part of the above elastic amplitude. They are associated with the unitarity diagrams with any number of totally open ladders modified by unopen ones. A typical example is given in Fig. 2. This can be viewed as a generalization of the conventional multiperipheral chain to multichain processes, modified by the unopen ladders. These unopen ladders lead to an absorption correction through which the s-channel unitarity is explicitly maintained. The main results of our calculations are the following:

(a) The total cross section has completely different high-energy behavior for the weak-coupling, the critical-coupling, and the strong-coupling case according to whether

$$\alpha(0)=\frac{g^2}{16\pi^2\mu^2}-1$$

is less than, equal to, or greater than one. (The coupling constant g is defined by $\mathcal{L}_I=-\frac{1}{6}g\varphi^3$, and μ is the meson mass.) In the first case the cross section goes to zero as $s\to\infty$. In the second, the total cross section approaches a constant. In the third case, however, the total cross section increases like $(\ln s)^2$ at large s, i.e., it saturates the Froissart bound.[14]

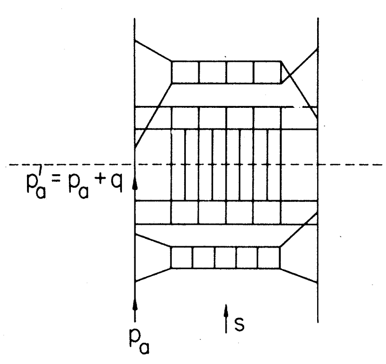

FIG. 2. Example of unitarity diagrams for a general production process in which two ladders are open. The solid lines cut by the dashed line correspond to the real final particles. On each side of the dashed line, permutation among the legs of open and unopen ladders is understood.

(b) The total, elastic, and inelastic cross sections σ_T, σ_E, and σ_I are the same as those obtained from an s-dependent absorption model:

$$\sigma_T=2\int d^2b(1-e^{-A(s,\vec{b})}),$$

$$\sigma_E=\int d^2b(1-e^{-A(s,\vec{b})})^2,$$

$$\sigma_I=\int d^2b(1-e^{-2A(s,\vec{b})}),$$

with $\vec{b}$ being the impact parameter and $A(s,\vec{b})$ an opaqueness given later. At large energy, and for the strong-coupling case, these cross sections reduce to

$$\sigma_E=\sigma_I=\tfrac{1}{2}\sigma_T=\pi b_m{}^2,$$

where $b_m=b_{\max}$ is found to be proportional to $\ln s$. These results agree with those in QED.[6] For the critical case, only a single ladder contributes at large s. It leads to a constant σ_T, and $\sigma_E\propto 1/\ln s$.

(c) The one-particle spectrum for a detected production particle with four-momentum k_μ is given by

$$d\sigma_1=\frac{g^6}{4\mu^4}\left(\frac{s}{\mu^2}\right)^{\overline{\alpha}(0)-1}\times\int\frac{d^2q}{(2\pi)^2}\,\frac{1}{(\vec{q}^2+\mu^2)^2[(\vec{k}+\vec{q})^2+\mu^2]^2}\,\frac{d^3k}{(2\pi)^3 2k^0},$$

with $\overline{\alpha}(0)=\alpha(0)$ for weak and critical coupling, $\overline{\alpha}(0)-1=[\alpha(0)-1]/[2\alpha(0)+3]$ for strong coupling. The s-dependent factor drops out for the critical case. The one-particle spectrum exhibits a dx/x distribution in the longitudinal momentum, and an s-independent transverse-momentum distribution.

(d) The number distribution function $P(n)$ for the strong-coupling inelastic processes is a superposition of Poisson distributions in the impact space:

$$P(n)=(\pi b_m{}^2)^{-1}\int d^2b\,e^{-B(s,\vec{b})}\frac{B(s,\vec{b})^n}{n!},$$

where $B(s,\vec{b})$ is related simply to the opaqueness $A(s,\vec{b})$, and has the same size b_m. The above distribution has a longer tail at large n than a single Poisson distribution. For weak and critical couplings, the number distribution is simply a Poisson distribution,

$$P(n)=\frac{\{[\alpha(0)+1]\ln(s/\mu^2)\}^n}{(s/\mu^2)^{\alpha(0)+1}n!}.$$

This paper is organized as follows: In Sec. II we describe our model in detail. The elastic amplitude is obtained, and so are the elastic and total cross sections. The existence of three distinctly different classes of solutions is demonstrated. We

TABLE I. A summary of various results.

	Weak coupling	Critical coupling	Strong coupling
σ_E, σ_I, σ_T	σ's $\to 0$	$\sigma_E \propto \frac{1}{\ln s}$ $\sigma_T \propto$ const	$\sigma_I = \sigma_E = \frac{1}{2}\sigma_T$ $\propto (\ln s)^2$
One-particle spectrum	Same as multiperipheral model: $s^{\alpha(0)-1} f(\vec{k}^2) \frac{d^3k}{k^0}$		
Multiparticle spectrum	Same as multiperipheral model: $s^{\alpha(0)-1} f(\vec{k}_1, \ldots, \vec{k}_n, s_{ij}) \prod_{l=1}^{n} \frac{d^3k_l}{k_l^0}$ s_{ij} = subenergy of particles i and j		Product of one-particle spectrum in $\vec{b}$ space
Correlation between particles	Some[a]		None
Number distribution	Poisson distribution[b]: $\frac{1}{n!}[\alpha(0)+1]^n \left(\ln\frac{s}{\mu^2}\right)^n \left(\frac{s}{\mu^2}\right)^{-\alpha(0)-1}$		Poisson in $\vec{b}$ space: $\int d^2b\, e^{-B(s,\vec{b})} B^n/n!$

[a]See Ref. 17.

[b]See Ref. 18.

then study the production processes in Sec. III. The inelastic amplitudes are obtained and the s-channel unitarity is verified. In Sec. IV we obtain many distribution properties for the production processes, such as one-particle or multiparticle spectra, the number distribution of the final particles, etc. The main results of this paper are summarized in Table I. In Sec. V we discuss the possible generalization and implications of our model calculation for hadron physics.

II. THE MODEL

To understand the motivation behind the present study of a φ^3-type coupling as a model for high-energy hadron scatterings, let us recall the main conclusions obtained in the recent work on high-order calculations in massive QED. Essentially there are two main points, namely, the eikonal representation of an elastic amplitude at high energies,[6,8] and the power dependence on s of the sum of the so-called "tower diagrams" of the elastic amplitude.[6,15]

The simplest example[6,7] of an eikonal amplitude in massive QED is obtained by summing to all orders the multiphoton exchanges in electron-electron scattering. The sum gives an elastic amplitude proportional to s and a constant total cross section as $s\to\infty$. If one considers the same set of diagrams in a scalar field theory with the electrons and the vector photons all replaced by spinless mesons, only the Born term survives and the total cross section vanishes as $s\to\infty$. This distinction between a vector and a spinless elementary-particle exchange, in these simple examples, somehow generates the incorrect impression that in field theory, exhange of elementary spin-1 particles is essential to have a nonvanishing total cross section at high energies, despite the well-known fact that higher spin can be produced by a composite system of two spinless particles.

Cheng and Wu[6] and Frolov *et al.*[15] have shown that by summing the so-called "tower diagrams" in massive QED, the forward elastic amplitudes at large s behave like

$$s^{1+(11/32\pi)\alpha^2}$$

with $\alpha = e^2/4\pi$. This result necessarily violates the Froissart bound. Later, it was found that this difficulty can be overcome by including those diagrams which are the s-channel iteration of this selected set of diagrams. The total cross section then saturates the Froissart bound, $(\ln s)^2$. It should be noticed that this saturation of the Froissart bound by the total cross section occurs for all nonvanishing values of the coupling constant, no matter how weak the interaction may be. This is somewhat disturbing since it leaves no room for the possibility of a *constant* total cross section at high energies, which is currently believed to be the true high-energy behavior for hadronic cross sections, although a logarithmic growth cannot be ruled out by the present empirical data.

It would be more interesting to have a model which is capable of producing an entirely different high-energy behavior for the scattering amplitudes and the cross sections, depending on the strength of coupling.

With these remarks in mind, we look into a scalar field theory with φ^3 coupling for a clue. It turns out that such a simple model has all the features we desire. It gives a nontrivial scattering amplitude as $s\to\infty$, and its high-energy behavior is different for different coupling strengths. We achieve these results by summing a certain class of diagrams to all orders, so that individually small terms add up to a nontrivial result. Another advantage of φ^3 theory is that, unlike the amplitudes in QED, there are no complicated γ matrices in the numerator functions. This simplification enables us not only to carry out with ease further calculations involving production processes, but also to see clearly the underlying physics. We believe that important physical consequences can be deduced much more efficiently from a model that does not involve complicated mathematics.

Our model is defined as follows. For the elastic-scattering amplitude we first sum the leading terms in each order of perturbation of the t-channel straight ladders, plus those obtained by interchange of the Mandelstam variables s and u. We then perform the s-channel iteration with the t-channel ladders as single units. In the s-channel iteration we have included all diagrams generated by permuting the legs of the ladders on the world lines of the incident particles. Thus the s-u crossing symmetry is maintained by the s-channel iteration. We make the further physical assumption that we only consider the integration regions in which the incident particles retain their large momenta during and after the scattering. As is pointed out in Ref. 8, this procedure leads to an eikonal form for the elastic amplitude with the t-channel ladder amplitude as the potential. For the inelastic production amplitude, we include all inelastic states which contribute to the absorptive part of the elastic amplitude. We find that the dominant contribution comes from diagrams with any number of totally open ladders modified by unopen ones. Each rung of the totally open ladders corresponds to a particle in the final inelastic states. The diagrams contributing to the elastic and inelastic scattering amplitudes are shown in Figs. 1 and 2, respectively.

The choice of the particular class of diagrams and particular regions of kinematics is based on simplicity considerations. As mentioned already, a t-channel ladder is the simplest structure which produces inelastic states. However, the sum of t-channel ladders alone violates the Froissart bound for sufficiently strong coupling. The minimum extension to preserve the Froissart bound is to perform the s-channel iteration in the manner described above. If we do not make the assumption that the incident particles retain their large momenta during the scattering, the results will be much more complicated. However, the corrections to our assumption can be understood at least qualitatively, and will be mentioned later.

The contribution due to the t-channel ladder diagrams is well known.[11] The leading term of the T matrix for the sum of a ladder and a crossed ladder with n rungs is

$$T_L^{(n)}(\vec{k}^2) = -i\pi g^2 \frac{[\alpha(\vec{k}^2)+1]^{n+1}[\ln(s/\mu^2)]^n}{s n!}, \qquad (2.1)$$

where

$$\alpha(\vec{k}^2)+1 = \frac{g^2}{4\pi}\int\frac{d^2q}{(2\pi)^2}\frac{1}{[(\vec{q}+\frac{1}{2}\vec{k})^2+\mu^2][(\vec{q}-\frac{1}{2}\vec{k})^2+\mu^2]}. \qquad (2.2)$$

We have followed the conventions used in Refs. 7 and 8 and work in the c.m. system. The large momenta of the incident particles are in the z direction, and the momentum transfer $\vec{k}$ is in the (1, 2) plane. The coupling constant g is defined through $\mathcal{L}_I = \frac{1}{6}g\varphi^3$, and μ is the meson mass. The above result can be obtained by the standard method as given in Ref. 4. In the following, we shall give an alternative derivation based on the infinite-momentum technique developed earlier, because it will help us to introduce our notations as well as to understand forthcoming calculations.

The amplitude for ladder and crossed-ladder diagrams with n rungs is (see Fig. 3)

$$T_L^{(n)} = i(ig)^{2(n+2)}\int\prod_{j=1}^{n+1}\frac{d^4q_j}{(2\pi)^4}\frac{i}{(p_a-q_1)^2-\mu^2+i\epsilon}\prod_{j=1}^{n}\left[\frac{i}{(q_j-q_{j+1})^2-\mu^2+i\epsilon}\,\frac{i}{q_j^{\,2}-\mu^2+i\epsilon}\,\frac{i}{(q_j+k)^2-\mu^2+i\epsilon}\right]$$
$$\times\frac{i}{q_{n+1}^{\;2}-\mu^2+i\epsilon}\,\frac{i}{(q_{n+1}+k)^2-\mu^2+i\epsilon}\left[\frac{i}{(q_{n+1}-p_b')^2-\mu^2+i\epsilon}+\frac{i}{(q_{n+1}+p_b)^2-\mu^2+i\epsilon}\right], \qquad (2.3)$$

where p_a and p_b are the initial momenta of particles a and b. Note that $\vec{p}_a=-\vec{p}_b$ lies on the z axis. The final momenta of the two particles, $\vec{p}_a'$ and $\vec{p}_b'$, are $\vec{p}_a+\vec{k}$ and $\vec{p}_b-\vec{k}$, respectively.

By a technique similar to that developed in Ref. 8, the leading contribution of (2.3) in the limit $s\to\infty$ can be easily extracted. The general procedure of that technique, adapted to the present case, is briefly sketched here.[16]

(1) Instead of the four-vector components p_μ,

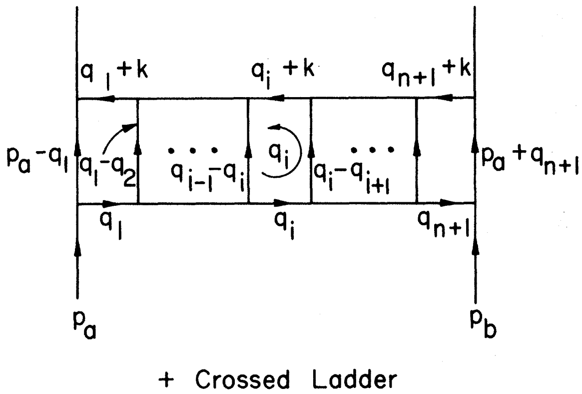

FIG. 3. Kinematics of a single ladder in detail.

we use the following combinations:

$$p_\pm = p^0 \pm p^3,$$

and the transverse components $p_{1,2}$ as our variables. The usefulness of the "+" and "−" combinations is that $p_\pm$ undergoes a simple scale change under a Lorentz transformation in the 3 direction, and integrations over either all p_+'s or all p_-'s automatically give results equivalent to the "infinite-momentum limit."

(2) For the straight ladder we carry out the q_- integrations by closing the contours from above. For leading contributions we only need to keep the poles

$$(q_j - q_{j+1})^2 - \mu^2 + i\epsilon = 0, \quad j = 0, 1, 2, \ldots n$$
$$q_0 = p_a. \tag{2.4}$$

These poles are in the upper half plane of $(q_{j+1})_-$, provided

$$p_{a+} = \sqrt{s} > q_{1+} > q_{2+} > \cdots > (q_{n+1})_+ > p_{b+} = \mu^2/\sqrt{s}. \tag{2.5}$$

Then

$$(q_{j+1})_- = q_{j-} - \frac{(\vec{q}_j - \vec{q}_{j+1})^2 + \mu^2}{(q_j - q_{j+1})_+} + i\epsilon. \tag{2.6}$$

Note that the ordering restriction (2.5) fails for small q_+ ($\lesssim \mu^2/\sqrt{s}$). However, these nonordering integration regions do not contribute to the leading ladder amplitude.[16]

(3) A further simplification follows from the observation that the dominant contribution from the q_+ integrations comes from the regions

$$p_{a+} = \sqrt{s} \gg q_{1+} \gg q_{2+} \gg \cdots \gg q_{n+} \gg p_{b+} = \mu^2/\sqrt{s}. \tag{2.7}$$

Thus, all the q_{i+}'s are only a very small fraction of $\sqrt{s}$,

$$\mu^2/\sqrt{s} \ll q_{i+} < \epsilon_i (q_{i-1})_+, \quad 0 < \epsilon_i \ll 1. \tag{2.8}$$

In the regions (2.7), the integrals decouple.

(4) The crossed ladder can be calculated similarly. Alternatively, it can be obtained from the straight ladder by the crossing substitution $s \to u \simeq -s$.

The sum of the straight and crossed ladders (2.3) now reduces to

$$T_L^{(n)}(k^2) = -i\frac{\pi}{s} g^2 \left(\frac{g^2}{4\pi}\right)^{n+1} \int_{\mu^2/\sqrt{s}}^{\sqrt{s}} \frac{dq_{1+}}{q_{1+}} \cdots \frac{dq_{n+}}{q_{n+}}$$
$$\times \left(\int \frac{d^2 q_i}{(2\pi)^2} \frac{1}{(\vec{q}_i^{\,2} + \mu^2)[(\vec{q}_i + \vec{k})^2 + \mu^2]} \right)^{n+1}. \tag{2.9}$$

The longitudinal phase-space integral in the region (2.7) can be easily worked out. It is

$$\int_{\mu^2/\sqrt{s}}^{\sqrt{s}} \frac{dq_{1+}}{q_{1+}} \int_{\mu^2/\sqrt{s}}^{q_{1+}} \frac{dq_{2+}}{q_{2+}} \cdots \int_{\mu^2/\sqrt{s}}^{(q_{n-1})_+} \frac{dq_{n+}}{q_{n+}}$$
$$= \frac{1}{n!} \int_{\mu^2/\sqrt{s}}^{\sqrt{s}} \frac{dq_{1+}}{q_{1+}} \cdots \frac{dq_{n+}}{q_{n+}}$$
$$= \frac{1}{n!} \left(\ln \frac{s}{\mu^2} \right)^n. \tag{2.10}$$

Putting this factor into (2.9), we obtain (2.1).

Note that in these integration regions a typical $q_+ q_-$ is small in comparison with $\vec{q}^{\,2} + \mu^2$, as can be readily verified by using (2.6) and (2.8). All the q_i's are then spacelike in these regions of interest. This is important for our later discussion to identify the possible inelastic states, as well as in verifying the s-channel unitarity.

It is easy to see that, to each order of perturbation series, the amplitude $T_L^{(n)}$ goes to zero like $s^{-1}[\ln(s/\mu^2)]^n$ at large s. However, after summing over all n, the resultant amplitude exponentiates to

$$T_L(\vec{k}^2) = -i\beta(\vec{k}^2)(s/\mu^2)^{\alpha(\vec{k}^2)}, \tag{2.11}$$

with

$$\beta(\vec{k}^2) = \pi g^2 [\alpha(\vec{k}^2) + 1]/\mu^2, \tag{2.12}$$

where an arbitrary scale factor μ^2 for the power of s has been inserted in (2.11) to make the dimensions on both sides correct. Its exact value can only be determined if the next leading terms are considered. If the coupling is very strong, the resultant amplitude can be very large at $s \to \infty$. In fact, it increases faster than s in the forward direction for $g^2/16\pi^2\mu^2 > 2$. Thus, for the strong-coupling case, the asymptotic behavior of the resultant amplitude has no resemblance at all to the individual terms in the perturbation calculation. The order-by-order perturbation analysis does not give us a clue to the behavior of the sum. Hence, additional information is needed for choosing a particular set of diagrams. This selected sum of diagrams, leading or nonleading alike, makes sense only after further physical justifications and interpretations are fed in.

At large coupling constant, the absorptive part of the ladder amplitude T_L will violate the Froissart bound $s(\ln s)^2$ imposed by the s-channel unitarity. One way of avoiding this difficulty is to perform the s-channel iteration with t-channel ladders as units. Under the assumption that the incident particles retain their large momenta during the scattering, the s-channel iteration of arbitrary connected pieces will exponentiate into an eikonal form, with the eikonal function being generated by the sum of all individual connected pieces. This result was proven in QED,[8] and can be generalized to φ^3 theory. Physically, this reflects the additivity of the eikonal function which, in many aspects, is equivalent to an effective potential.

Hence, the s-channel iteration of these ladders leads to the standard eikonal form

$$T_E(s,\vec{k}^2)=-2is\int d^2b\, e^{-i\vec{k}\cdot\vec{b}}(1-e^{-A(s,\vec{b})}), \tag{2.13}$$

where

$$A(s,\vec{b})=-i\chi(s,\vec{b})$$

in our model is given by

$$A(s,\vec{b})=\frac{1}{2s}\int\frac{d^2k}{(2\pi)^2}\,e^{i\vec{k}\cdot\vec{b}}\beta(\vec{k}^2)\left(\frac{s}{\mu^2}\right)^{\alpha(\vec{k}^2)}$$

$$=\frac{\pi g^2}{2s\mu^2}\int\frac{d^2k}{(2\pi)^2}\,e^{i\vec{k}\cdot\vec{b}}[\alpha(\vec{k}^2)+1]\left(\frac{s}{\mu^2}\right)^{\alpha(\vec{k}^2)}. \tag{2.14}$$

The "potential" (or the eikonal function) χ given by Eq. (2.14) is purely imaginary. Thus, our model is an absorption model, and the elastic amplitude is dominated by its imaginary part.

Once the elastic amplitude is known, one can compute the elastic cross section, and through the optical theorem, the total cross section. The differential elastic cross section is

$$d\sigma_E=\frac{1}{v_{ab}}\frac{1}{2E_a2E_b}\,|T_E|^2\,\frac{d^3p_a'}{2E_a'(2\pi)^3}\,\frac{d^3p_b'}{2E_b'(2\pi)^3}$$

$$\times(2\pi)^4\delta^4(p_a'+p_b'-P), \tag{2.15}$$

where p_a' and p_b' are the momenta of the final particles a and b, and ($P^0=\sqrt{s}$, $P^i=0$) is the total momentum. After integrating out $\delta^4(p_a'+p_c'-P)$ and making use of $v_{ab}=2$, we have

$$d\sigma_E=\frac{1}{4s^2}\,|T_E|^2\,\frac{d^2k}{(2\pi)^2}, \tag{2.16}$$

where $\vec{k}$ is the (transverse) momentum transfer. Substituting Eq. (2.13) into Eq. (2.16) and carrying out the $\vec{k}$ integration, we have the total elastic cross section in our model:

$$\sigma_E=\int\frac{d^2k}{(2\pi)^2}\left|\int d^2b\,e^{-i\vec{k}\cdot\vec{b}}(1-e^{-A(s,\vec{b})})\right|^2$$

$$=\int d^2b(1-e^{-A(s,\vec{b})})^2, \tag{2.17}$$

where we have extended the range of integration, $0<\vec{k}^2<s$, to $0<\vec{k}^2<\infty$. The error introduced is negligible. The total cross section, obtained from the optical theorem, is

$$\sigma_T=-\frac{1}{s}\,\mathrm{Im}\,T_E(s,\vec{k}=0)=2\int d^2b(1-e^{-A(s,\vec{b})}), \tag{2.18}$$

and the total inelastic cross section is

$$\sigma_I=\sigma_T-\sigma_E=\int d^2b(1-e^{-2A(s,\vec{b})}). \tag{2.19}$$

In the next section we shall study the inelastic processes as well, and verify that the total inelastic cross section, as a sum of contributions from all channels, is indeed given by Eq. (2.19). The explicit verification of Eq. (2.19) is an important consistency check on our model and our approximation used. The three relations (2.17), (2.18), and (2.19) are a more detailed check of unitarity than the Froissart bound, which only sets an upper limit on the growth of the total cross section.

Before we analyze the production processes, let us study the total cross sections given in (2.17)–(2.19). It is important to notice that the absorptive potential $A(s,\vec{b})$ will lead to different asymptotic s dependence of the cross sections as the coupling constant increases. Three cases are noted: for $\alpha(0)$ $(=g^2/16\pi^2\mu^2-1)>1$, $=1$, or <1. We shall discuss their properties according to increasing coupling strength.

(a) $\alpha(0)<1$. This is the weak-coupling case. The potential $A(s,\vec{b})$ approaches zero at large s as a negative power of s. Consequently, the total cross section approaches zero as

$$\sigma_T\approx\sigma_I\approx\frac{\beta(0)}{\mu^2}\left(\frac{s}{\mu^2}\right)^{\alpha(0)-1},$$

$$\sigma_E\propto\left(\frac{s}{\mu^2}\right)^{2[\alpha(0)-1]}\frac{1}{\ln s}.$$

(b) $\alpha(0)=1$, the critical-coupling case. The asymptotic behavior of $A(s,\vec{b})$ is determined by the small $\vec{k}^2$ integration region in (2.14), where $\alpha(\vec{k}^2)\approx 1-c\vec{k}^2$ with $c=1/3\mu^2$. $A(s,\vec{b})$ can be computed as

$$A(s,\vec{b}) = \frac{1}{2s}\int \frac{d^2k}{(2\pi)^2}\, e^{i\vec{k}\cdot\vec{b}}\beta(\vec{k}^2)\left(\frac{s}{\mu^2}\right)^{\alpha(\vec{k}^2)}$$

$$\approx \frac{\beta(0)}{2\mu^2}\int \frac{d^2k}{(2\pi)^2}\, e^{i\vec{k}\cdot\vec{b}}\, e^{-c\ln(s/\mu^2)\vec{k}^2}$$

$$= \frac{\beta(0)}{8\pi c\mu^2 \ln(s/\mu^2)}\, e^{-\vec{b}^2/4c\ln(s/\mu^2)}$$

$$= \frac{24\pi^2}{\ln(s/\mu^2)}\exp\left[-\frac{3\mu^2}{4\ln(s/\mu^2)}\vec{b}^2\right]. \quad (2.20)$$

Even though $A(s,\vec{b})\to 0$ at $s\to\infty$ as before, the integrated total cross section approaches a constant:

$$\sigma_T = 2\int d^2b(1-e^{-A(s,\vec{b})}) \approx 2\int d^2b A(s,\vec{b})$$

$$= \beta(0)/\mu^2 = 64\pi^3/\mu^2. \quad (2.21)$$

The absorption range is $b_m \sim [\ln(s/\mu^2)]^{1/2}/\mu$. The elastic cross section, on the other hand, vanishes like $1/\ln s$,

$$\sigma_E = \int d^2b(1-e^{-A(s,\vec{b})})^2 \approx \int d^2b[A(s,\vec{b})]^2$$

$$= \frac{\beta(0)^2}{32\pi c\mu^4\ln(s/\mu^2)} = \frac{384\pi^5}{\ln(s/\mu^2)\mu^2}. \quad (2.22)$$

This particular s dependence of σ_E is a consequence of the fact that the height of the elastic peak is s-independent, while its width shrinks logarithmically with s.

(c) $\alpha(0)>1$, the strong-coupling case. The elastic amplitude in this case has completely different nature from those in the previous two cases. The absorptive potential $A(s,\vec{b})$ becomes very strong at small b, and falls off to zero rapidly

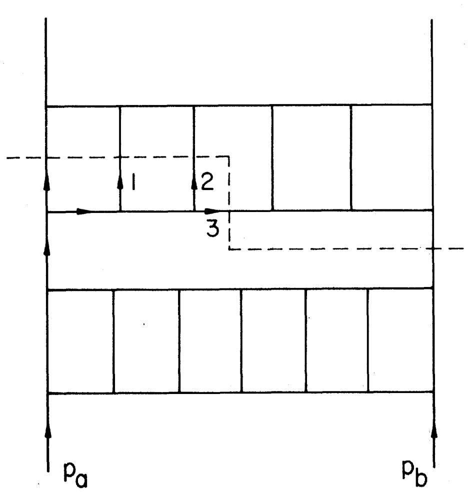

FIG. 4. Example of a unitarity diagram which does not contribute to the production process. The dashed line represents the unitarity cut.

when $b=|\vec{b}|$ becomes larger than its size $b_m \sim \ln s$. This is similar to the results obtained by Cheng and Wu based on QED calculations.[6] Nevertheless, their results predict a large amplitude for *all* coupling constants no matter how weak the coupling constant α is.

To compute the asymptotic behavior of $A(s,\vec{b})$ at large s, we find that, just as in the critical-coupling case, the important contribution of the integral (2.14) comes from the region of small $\vec{k}^2 \sim \mu^2/\ln(s/\mu^2)$. In this region of small $\vec{k}$, we can approximate $\alpha(\vec{k}^2)$ by $\alpha(0) - c\vec{k}^2$ with

$$c = \alpha'(t=0) = g^2/96\pi^2\mu^4. \quad (2.23)$$

Hence

$$A(s,\vec{b}) \approx \frac{1}{2s}\int \frac{d^2k}{(2\pi)^2}\, e^{i\vec{k}\cdot\vec{b}}\beta(0)\left(\frac{s}{\mu^2}\right)^{\alpha(0)-c\vec{k}^2}$$

$$= \frac{\beta(0)}{8\pi c\mu^2\ln(s/\mu^2)}\left(\frac{s}{\mu^2}\right)^{\alpha(0)-1} e^{-b^2/4c\ln(s/\mu^2)}$$

$$= \frac{\beta(0)}{8\pi c\mu^2\ln(s/\mu^2)}$$

$$\times\exp\left[[\alpha(0)-1]\ln\frac{s}{\mu^2}\left(1-\frac{b^2}{b_m{}^2}\right)\right], \quad (2.24)$$

with

$$b_m{}^2 = 4c[\alpha(0)-1][\ln(s/\mu^2)]^2$$

$$= (g^2/24\pi^2\mu^4)(g^2/16\pi^2\mu^2 - 2)[\ln(s/\mu^2)]^2. \quad (2.25)$$

Results similar to (2.24) and (2.25) can be obtained more rigorously by the method of steepest descent. It gives an identical result for $\alpha(0)\approx 1$, and leads to a slightly different coefficient in (2.24) when $\alpha(0)>1$. For our purposes, Eqs. (2.24) and (2.25) are accurate enough for all future discussions. If $b/b_m<1$, $A(s,\vec{b})$ is seen to increase as a power of s. Hence it corresponds to an infinitely strong absorption. In this case, we can approximate the attenuation factor e^{-A} by zero. On the other hand, if $b/b_m>1$, the absorption potential $A(s,\vec{b})$ acquires a negative power of s and vanishes rapidly at large s. Then we can approximate e^{-A} by 1, or $1-e^{-A}$ by zero. Thus, $e^{-A(s,b)} \approx \theta(b/b_m - 1)$. This indicates that the target at large s is completely absorptive for $b/b_m<1$, and completely transparent for $b/b_m>1$. The quantity b_m describes the size of the absorption disk. In the present case, b_m increases as $\ln s$, as was demonstrated by Froissart for a strong s-dependent potential.[14]

Now we can compute σ_E and σ_T for the strong-coupling case easily. Using

$$e^{-A}=\theta(b/b_m-1),\quad 1-e^{-A}=\theta(1-b/b_m), \tag{2.26}$$

we have, through Eqs. (2.17)–(2.19),

$$\sigma_E=\sigma_I=\tfrac{1}{2}\sigma_T=\pi b_m{}^2. \tag{2.27}$$

These results agree with similar massive-QED calculations.[6]

III. PRODUCTION PROCESSES

The study of inelastic processes is important for at least two reasons. First, in addition to the total and elastic cross sections, it supplies further information about multiplicity, one-particle and multiparticle spectra, number distributions, etc. Second, it provides a consistency check of the approximation scheme employed, since inelastic processes are related to the imaginary part of the forward elastic amplitude by the optical theorem. So far a field-theoretic description for both elastic and inelastic high-energy scattering is still lacking, since the existing calculations have been confined primarily to the elastic amplitude. The results for production processes derived from a simple class of diagrams studied in this and the next sections, together with those for elastic scattering obtained in previous sections, represent our attempt to supply such a more detailed picture for these high-energy elastic and inelastic processes.

The inelastic states which contribute to the absorptive part of the elastic amplitude can be determined by all possible unitarity cuts. Under the approximation of keeping only the leading $(\ln s)^N$ terms in the ladder amplitudes, the inelastic states are rather simple. They correspond to opening up completely any number of ladders modified by unopen ones. A typical diagram is shown in Fig. 2. Under the leading $(\ln s)^N$ approximation for computing a t-channel ladder, it was pointed out in the previous section that the sides of a ladder carry only spacelike momenta, and hence cannot be realized as real physical particles. Thus, a unitarity diagram such as Fig. 4, which cuts through only part of a ladder, does not contribute, because it has to cut through its side at least once. Actually, the vanishing of this type of contribution follows directly from our assumption that the incident particles retain their large momenta during the scattering. By cutting only a part of a ladder, one makes it necessary to supply these intermediate particles (particles 1, 2, and 3, in Fig. 4) with a finite fraction of the large incident momentum p_a. Hence these processes should be excluded. This conclusion is rather general, and is not restricted to ladder diagrams.

The T-matrix amplitude for a typical production process as in Fig. 5(a) is

$$\begin{aligned}
T_{\text{Fig. 5(a)}}=i2s\int\prod_{i=1}^{6}\frac{dq_{i-}}{2\pi}\,2\pi\delta\Big(\sum q_{i-}\Big)&\prod_{\substack{\text{all propagators}\\ \text{along particle } a}}\frac{i\sqrt{s}}{(p_a+\sum q)^2-\mu^2+i\epsilon}\\
\times\int\prod_{i=1}^{6}\frac{dq'_{i+}}{2\pi}\,2\pi\delta\Big(\sum q'_{i+}\Big)&\prod_{\substack{\text{all propagators}\\ \text{along particle } b}}\frac{i\sqrt{s}}{(p_b-\sum q')^2-\mu^2+i\epsilon}\\
\times\int\prod_{i=1}^{4}\frac{d^2l_i}{(2\pi)^2}\,(2\pi)^2\delta\Big(\sum\vec{l}_i-\vec{q}\Big)&\\
\times\left(\frac{-i}{2s}\right)M(s,\vec{l}_1;k'_{(1)}s)\left(\frac{-i}{2s}\right)M(s,\vec{l}_2;k'_{(2)}s)&\left(-\frac{i}{s}\right)T_{L1}(s,\vec{l}_3)\left(-\frac{i}{s}\right)T_{L2}(s,\vec{l}_4),
\end{aligned} \tag{3.1}$$

with

$$\vec{l}_3=\vec{q}_3+\vec{q}_4,\quad \vec{l}_4=\vec{q}_5+\vec{q}_6, \tag{3.2}$$

where T_L is the ladder amplitude with momentum transfer $\vec{l}$ given in (2.9), and

$$M(s,\vec{l};k_1,\ldots,k_n)=i(ig)^{n+2}\,\frac{i}{l^2-\mu^2+i\epsilon}\times\cdots\times\frac{i}{(l+k_1+\cdots+k_n)^2-\mu^2+i\epsilon} \tag{3.3}$$

is the multiperipheral amplitude [see Fig. 5(b)]. Equation (3.1) is very complicated and it requires some explanation. The amplitude for Fig. 5(a) in the form (3.1), as written, is obtained from the standard Feynman rules by noting the following:

(1) In the kinematic regions of interest a momentum transfer $\vec{q}$ to or from the energetic lines corresponding to the incident particles is almost transverse, and all the secondary particles carry only negligibly small fractions of the incident momenta. Thus we can write

$$(2\pi)^4\delta^4(\sum q_i - q) \approx 2(2\pi)\delta(\sum q_{i-})(2\pi)\delta(\sum q_{i+})(2\pi)^2\delta^2(\sum \vec{q}_i - \vec{q})$$

$$\approx 2(2\pi)\delta(\sum q_{i-})(2\pi)\delta(\sum q'_{i+})(2\pi)^2\delta^2(\sum \vec{l}_i - \vec{q}).$$

(2) The amplitude for a single straight ladder plus the crossed one can be given a simple representation. Let us write (2.3) as

$$T_L^{(n)} = i(ig)^4 \frac{1}{2s} \int \frac{d^4q_1}{(2\pi)^4} \frac{d^4q'_1}{(2\pi)^4} \left[\frac{i\sqrt{s}}{(p_a - q_1)^2 - \mu^2 + i\epsilon} + \frac{i\sqrt{s}}{(p'_a + q_1)^2 - \mu^2 + i\epsilon} \right]$$

$$\times \frac{i}{q_1^2 - \mu^2} \frac{i}{q_2^2 - \mu^2} B_n(q_1 q_2, q'_1 q'_2) \frac{i}{q_1'^2 - \mu^2} \frac{i}{q_2'^2 - \mu^2} \left[\frac{i\sqrt{s}}{(p_b + q'_1)^2 - \mu^2 + i\epsilon} + \frac{i\sqrt{s}}{(p'_b - q'_1)^2 - \mu^2 + i\epsilon} \right],$$

where we have exhibited explicitly only the dependence of the amplitude on the legs $q_{1,2}$ and $q'_{1,2}$ attached to the incident-particle lines p_a and p_b. All the other loop integrals are collectively represented by the single function $B_n(q_1q_2, q'_1q'_2)$. Now, as $s \to \infty$ we have

$$\frac{i\sqrt{s}}{(p_a - q_1)^2 - \mu^2 + i\epsilon} + \frac{i\sqrt{s}}{(p'_a + q_1)^2 - \mu^2 + i\epsilon} \to \frac{i\sqrt{s}}{-p_{a+}q_{1-} + i\epsilon} + \frac{i\sqrt{s}}{p_{a+}q_{1-} + i\epsilon} = 2\pi\delta(q_{1-}),$$

and similarly,

$$\frac{i\sqrt{s}}{(p_b + q'_1)^2 - \mu^2 + i\epsilon} + \frac{i\sqrt{s}}{(p'_b - q'_1)^2 - \mu^2 + i\epsilon} \to 2\pi\delta(q'_{1+}).$$

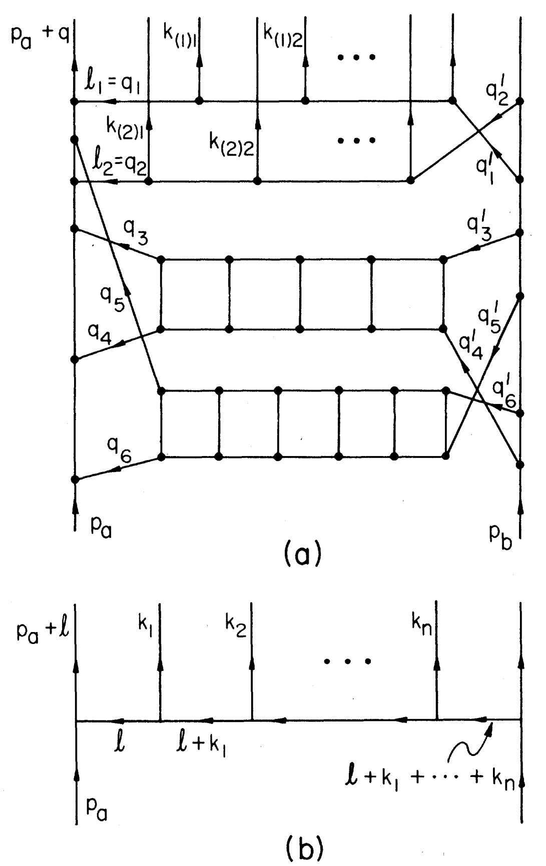

FIG. 5. (a) Kinematics of a typical production amplitude in detail. The dots represent point φ^3 vertices. (b) Kinematics of an open ladder in detail.

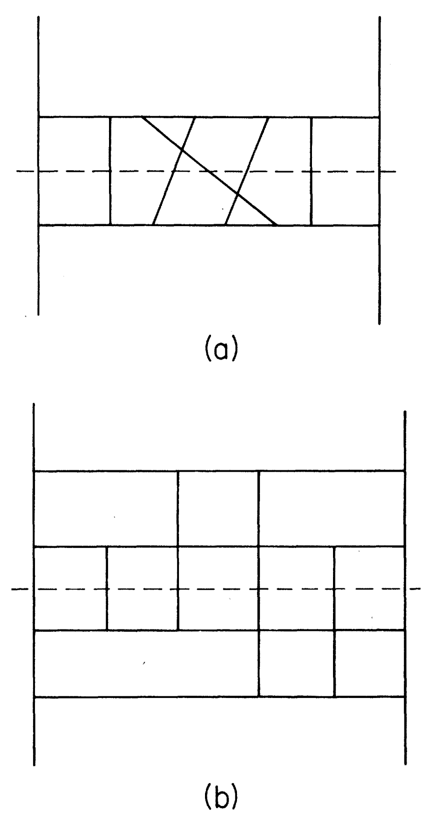

FIG. 6. (a) A ladder with crossed rungs produced by squaring the production amplitude of Fig. 5(a). (b) Interference between two ladders produced by squaring the production amplitude of Fig. 5(a).

Thus we obtain finally

$$T_L^{(n)} = i(ig)^4 \frac{1}{2s} \int \frac{d^2q_1}{(2\pi)^2} \frac{d^2q_1'}{(2\pi)^2} \frac{1}{(\vec{q}_1{}^2+\mu^2)} \frac{1}{(\vec{q}_2{}^2+\mu^2)} \frac{1}{(\vec{q}_1'^2+\mu^2)} \frac{1}{(\vec{q}_2'^2+\mu^2)} \int \frac{dq_{1+}}{4\pi} \frac{dq_{1-}'}{4\pi} B_n(q_1q_2, q_1'q_2')\bigg|_{q_{1-}=q_{1+}'=0} . \tag{3.4}$$

In (3.4), the limit of the dq_{1+} and dq_{1-}' integrations is restricted to $(-\sqrt{s}, \sqrt{s})$. This integration limit reflects the total available longitudinal phase spaces, and is crucial for the understanding of the $(\ln s)^N$ factors appearing in the ladder amplitude. This point was discussed in the first paper of Ref. 8, and will be clarified in more detail in a forthcoming paper.

(3) In the amplitude for Fig. 5(a) we collect together the q_{i-} (q_{i+}') integrations for the left (right) loops attached to the fast-moving lines and the corresponding propagators for the fast-moving line segments. The remaining factors in the amplitude can then be identified as a product of the amplitudes associated with single ladders, (3.4) or (2.6), and the multiperipheral diagrams. This gives (3.1). In doing so we have anticipated the result that all the q_{i-}'s and q_{i+}''s are small by the δ functions produced when all permutations of the legs are included (see below). A simplified result can be obtained if we include all other diagrams with the same final states. Within our model, this means that for a given set of open and unopen ladders, we include diagrams obtained by permuting the legs of these ladders attached to the incident-particle lines a and b. The sum of these diagrams results in the total cancellation of the principle parts in the propagators along the incident lines. Hence, the first two integrals in (3.1) reduce simply to $1/2^N = \frac{1}{4}$, since as $s\to\infty$,

$$\sum_{\text{permutations}} \int \prod_{i=1}^{N} \frac{dq_{i-}}{2\pi} 2\pi\delta\Big(\sum q_{i-}\Big) \prod \frac{i\sqrt{s}}{(p_a+\sum q)^2-\mu^2+i\epsilon}$$
$$\times \int \prod_{i=1}^{N} \frac{dq_{i+}'}{2\pi} 2\pi\delta\Big(\sum q_{i+}'\Big) \prod \frac{i\sqrt{s}}{(p_b-\sum q')^2-\mu^2+i\epsilon} = \frac{1}{2^N},$$

where N is the number of ladders exchanged. This factor $1/2^N$ arises from the overcounting due to the two-fold symmetry of a ladder under reflection, if we permute at the same time all the legs attached to the line a *and* the legs attached to the right line b. Equation (3.1) now simplifies to

$$T_{\text{with all perm.}} = i2s \int \prod \frac{d^2l_i}{(2\pi)^2} (2\pi)^2\delta^2\Big(\sum \vec{l}_i - \vec{q}\Big)\Big(-\frac{i}{2s}\Big)M_1(s,\vec{l}_1)$$
$$\times \Big(-\frac{i}{2s}\Big)M_2(s,\vec{l}_2)\Big(-\frac{i}{2s}\Big)T_{L1}(s,\vec{l}_3)\Big(-\frac{i}{2s}\Big)T_{L2}(s,\vec{l}_4)$$
$$= i2s\int d^2b\, e^{-i\vec{q}\cdot\vec{b}}\Big(-\frac{i}{2s}\Big)\tilde{M}_1(s,\vec{b})\Big(-\frac{i}{2s}\Big)\tilde{M}_2(s,\vec{b})\Big(-\frac{i}{2s}\Big)\tilde{T}_{L1}(s,\vec{b})\Big(-\frac{i}{2s}\Big)\tilde{T}_{L2}(s,\vec{b}), \tag{3.5}$$

where $\tilde{M}$ and $\tilde{T}$ are Fourier transforms of M and T, $M(s,\vec{l})$ and $M(s,\vec{b})$ are shorthand notations for $M(s,\vec{l};k_1...k_n)$ and $M(s,\vec{b};k_1,...,k_n)$. It is tacitly assumed that all the ladders are different in Fig. 5(a), to obtain (3.5). This can be readily generalized to include diagrams with N_1 ladders of the first kind, N_2 of the second kind, etc., being exchanged. An additional factor $1/N_1!N_2!\cdots$ will appear with

$$T_{(N_1,N_2,\ldots)} = i2s\int d^2b\, e^{-i\vec{q}\cdot\vec{b}}\Big(-\frac{i}{2s}\Big)\tilde{M}_1(s,\vec{b})\Big(-\frac{i}{2s}\Big)\tilde{M}_2(s,\vec{b})$$
$$\times\frac{1}{N_1!}\Big[-\frac{i}{2s}\tilde{T}_{L_1}(s,\vec{b})\Big]^{N_1}\frac{1}{N_2!}\Big[-\frac{i}{2s}\tilde{T}_{L_2}(s,\vec{b})\Big]^{N_2}\times\cdots. \tag{3.6}$$

Summing over all possible sets of N_i's, we obtain the amplitude for N open ladders,

$$T(s,\vec{q};\{k\}) = \sum_{\{N_i\}} T_{(N_1,N_2,\ldots)}$$
$$= i2s\int d^2b\, e^{-i\vec{q}\cdot\vec{b}}\Big[\prod_{i=1}^{N}\Big(-\frac{i}{2s}\Big)\tilde{M}_i(s,\vec{b})\Big]e^{-A(s,\vec{b})}, \tag{3.7}$$

where, from (2.13),

$$A(s,\vec{b})=\sum_n \frac{i}{2s}\,\tilde{T}_L^{(n)}(s,\vec{b}). \tag{3.8}$$

Note that $M(s,\vec{b})$ depends also on the final-state momenta $\{k\}$, which are suppressed for notational simplicity. From (3.7) it is seen that the production processes with an arbitrary number of unopen ladders can be obtained in $\vec{b}$ space from the simple multiperipheral processes by including an absorption correction. Furthermore, $A(s,\vec{b})$ is the absorptive part of the multiperipheral amplitude. Thus, the absorptive potential $A(s,\vec{b})$ appearing in the correction factor is generated precisely from the same mechanism which leads to the inelastic processes. For a process in which the nonleading $(\ln s)^N$ terms or some more general classes of diagrams are included, the eikonal function $\chi(s,\vec{b})$ is no longer purely imaginary. However, equations analogous to (3.7) are still valid, and now only the absorptive part of $\chi(s,\vec{b})$ is given by the inelastic processes. The details of this result will be discussed in Sec. IV and in future publications.

From the inelastic amplitude (3.7), we can calculate the differential inelastic cross section by squaring the amplitude and including proper phase-space factors. However, when we square the matrix element, we include not only the unitarity diagrams given in Fig. 2, but diagrams with crossed rungs [Fig. 6(a)] and mixed ladders [Fig. 6(b)] as well. Nevertheless, diagrams with crossed rungs do not contribute to leading $(\ln s)^N$ behavior, and the mixed-ladder diagrams correspond to exchange of different kinds of connected pieces. To be consistent with the class of diagrams studied in the elastic amplitude, these extra terms should not be included. They should be considered in connection with exchanges of other types of connected pieces. Moreover, these additional terms correspond to the interference between one ladder contribution and another. Since the interference terms do not have a definite sign, they tend to cancel each other when all interference terms are included. Neglect of these terms is a kind of random-phase approximation. Since we are only interested in the leading contribution and the general feature of the theory, we shall ignore these interference terms, and other types of connected pieces. As we shall see in the final forms, the neglect of these terms does not lead to any formal inconsistency as far as the leading $(\ln s)^N$ terms are concerned.

Hence, we only consider those processes in which the two halves of each open ladder rejoin together in the unitarity diagram to give a simple ladder. In this way we obtain the differential inelastic cross section as

$$d\sigma=\frac{1}{2s}\,|T|^2\times(\text{phase-space factor}). \tag{3.9}$$

If one does not measure the momenta of the fast-moving particles a and b, the phase-space factor (P.S.F.) in Eq. (3.9) reduces to

$$\begin{aligned}\text{P.S.F.}&=\frac{d^3p_a'}{(2\pi)^3 2E_a'}\,\frac{d^3p_b'}{(2\pi)^3 2E_b'}\prod_{i=1}^{n}\frac{d^3k_i}{(2\pi)^3 2k_i^0}\,(2\pi)^4\delta^4\left(p_a'+p_b'+\sum_{i=1}^{n}k_i-p_a-p_b\right)\\&\to\frac{1}{2s}\,\frac{d^2q}{(2\pi)^2}\prod_{i=1}^{n}\frac{d^3k_i}{(2\pi)^3 2k_i^0}\,.\end{aligned} \tag{3.10}$$

So we have

$$\begin{aligned}d\sigma&=\frac{1}{(2s)^2}\int\frac{d^2q}{(2\pi)^2}\,|T(s,\vec{q};\{k\})|^2\prod\frac{d^3k}{(2\pi)^3 2k^0}\\&=\int d^2b\,e^{-2A(s,\vec{b})}\prod_{\substack{i=1\\ \text{(over the ladder)}}}^{N}\left|\frac{1}{2s}\,\tilde{M}_i(s,\vec{b},\{k_i\})\right|^2\prod_{\text{all } j}\frac{d^3k_j}{(2\pi)^3 2k_j^0}\,,\end{aligned} \tag{3.11}$$

where N is the number of open ladders. The integration regions of d^3k are restricted by

$$\epsilon\sqrt{s}\geq k_j^0,\quad 1\gg\epsilon>0. \tag{3.12}$$

This restriction is imposed by the requirement that the large momenta in particles a and b do not change during the scattering. This restriction is satisfied automatically for leading $(\ln s)^N$ terms in the cross section. An interesting feature of (3.11) is that the k integrations associated with different ladders are completely decoupled in $\vec{b}$ space, and can be evaluated independently.

The contribution due to a single open ladder with n rungs is [Fig. 5(b)]

$$\int \prod \frac{d^3k_j}{(2\pi)^3 2k_j^0} \left| \frac{1}{2s} \tilde{M}(s, \vec{b}; \{k_j\}) \right|^2$$

$$= \frac{1}{(2s)^2} \int \frac{d^2q}{(2\pi)^2} \frac{d^2q'}{(2\pi)^2} e^{i(\vec{q}-\vec{q}')\cdot\vec{b}} \int \prod_j \frac{d^3k_j}{(2\pi)^3 2k_j^0} M(s, \vec{q}; k_j) M^*(s, \vec{q}'; k_j)$$

$$= \frac{1}{(2s)^2} g^{2(n+2)} \int \frac{d^2q}{(2\pi)^2} \frac{d^2q'}{(2\pi)^2} e^{i(\vec{q}-\vec{q}')\cdot\vec{b}} \int \prod \left(\frac{d^3k}{(2\pi)^3 2k^0}\right) \frac{1}{(q^2 - \mu^2 + i\epsilon)(q'^2 - \mu^2 + i\epsilon)}$$

$$\times \frac{1}{[(q+k_1)^2 - \mu^2 + i\epsilon][(q'+k_1)^2 - \mu^2 + i\epsilon]} \times \cdots \times \frac{1}{[(q+k_1+\cdots+k_n)^2 - \mu^2 + i\epsilon][(q'+k_1+\cdots+k_n)^2 - \mu^2 + i\epsilon]}. \tag{3.13}$$

The leading term is, with the help of (2.3) and (2.9),

$$\frac{4\pi g^2}{(2s)^2} \frac{1}{n!} \left(\ln \frac{s}{\mu} \right)^n \int \frac{d^2\Delta}{(2\pi)^2} e^{i\vec{\Delta}\cdot\vec{b}} [\alpha(\vec{\Delta}^2) + 1]^{n+1} = \frac{1}{s} i\tilde{T}_L^{(n)}(s, \vec{b}). \tag{3.14}$$

If we sum over n, the one-ladder contribution finally reduces to

$$\frac{1}{s} i \sum \tilde{T}_L^{(n)}(s, \vec{b}) = 2A(s, \vec{b}). \tag{3.15}$$

After substituting (3.15) into (3.11) and inserting a correction factor $1/N!$ for all possible orderings of the open ladders, we find that the total inelastic cross section due to N open ladders is

$$\sigma^{(N)} = \frac{1}{N!} \int d^2b\, e^{-2A(s,\vec{b})} [2A(s, \vec{b})]^N. \tag{3.16}$$

Therefore the total inelastic cross section is

$$\sigma_I = \sum_{N=1}^{\infty} \sigma^{(N)} = \int d^2b\, e^{-2A}(e^{2A} - 1) = \int d^2b (1 - e^{-2A(s,\vec{b})}), \tag{3.17}$$

and consequently, the total cross section is

$$\sigma_T = \sigma_E + \sigma_I = 2\int d^2b (1 - e^{-A(s,\vec{b})}). \tag{3.18}$$

The results obtained here agree with those obtained from the optical theorem in Eqs. (2.18) and (2.19). This is a direct check of forward s-channel unitarity. As we have seen, the presence of the absorptive correction factor $e^{-A(s,\vec{b})}$ in (3.7) is crucial for the resultant amplitude to obey the s-channel unitarity and Froissart bound. Thus, the larger the production amplitude $A(s, \vec{b})$ appearing in (3.16), the larger will be the absorption correction $e^{-A(s,\vec{b})}$. The inelastic contribution can never violate unitarity and the Froissart bound for any coupling strength.

We conclude this section by pointing out that the inelastic states studied in this model obey not only the forward ($t=0$) s-channel unitarity in the form of the optical theorem, but also the nonforward (but with finite t) s-channel unitarity

$$\frac{1}{i}(T_{fi} - T_{fi}^\dagger) = -\sum_n \left[T_{fn}^\dagger T_{ni} \prod_{l\in\{n\}} \frac{d^3p_l}{(2\pi)^3 2p_l^0} (2\pi)^4 \delta\left(\sum p_l - p_i\right)\right]$$

$$= -\sum_n [(T_{nf})^* T_{ni} \times (\text{phase-space factor})] \tag{3.19}$$

as well.

To see how various terms work out, we first compute the contribution of (3.19) due to the elastic channel (Fig. 7). It gives

$$[\text{r.h.s. of } (3.19)]_{\text{elastic channel}} = -2s \int d^2b\, e^{-i(\vec{l}-\vec{q})\cdot\vec{b}} (e^{-A(s,\vec{b})} - 1) 2s \int d^2b'\, e^{-i\vec{q}\cdot\vec{b}'} (e^{-A(s,\vec{b}')} - 1)$$

$$\times \frac{d^3p_a''}{(2\pi)^3 E_a''} \frac{d^3p_b''}{(2\pi)^3 2E_b''} (2\pi)^4 \delta^4(p_a'' + p_b'' - p_a - p_b), \tag{3.20}$$

where $\vec{1}$ is the momentum transfer in the elastic amplitude (2.13). After integrating out dp_{a+}'', dp_{b-}'', and $d^2(p_a''+p_b'')$, we find that the phase-space factor in (2.20) reduced to $(1/2s)\, d^2q/(2\pi)^2$. Hence, (3.20) becomes

$$[\text{r.h.s. of } (3.19)]_{\text{elastic channel}} = -2s \int d^2b\, e^{-i\vec{1}\cdot\vec{b}}(e^{-A(s,\vec{b})}-1)^2. \tag{3.21}$$

Next, we compute the inelastic contribution due to N open ladders. The phase-space factor in this case, after the momenta of the incident lines p_a'' and p_b'' have been integrated out, is given by (3.10). Analogously to the d^3k_i integrals in (3.11), the k-integration regions are restricted by $\epsilon\sqrt{s} > k_i^0$. Making use of (3.7) and (3.10), we have

$$\begin{aligned}
[\text{r.h.s of } (3.19)]_{N\text{ open ladders}} &= -\frac{1}{2s}\int \frac{d^2q}{(2\pi)^2} \sum_{\text{all }\{n_i\}} \left[\prod_i \frac{d^3k_i}{(2\pi)^3 2k_i^0}\, T(s, \vec{q}-\vec{1}, \{k\})^* T(s, \vec{q}, \{k\})\right] \\
&= -2s \int \frac{d^2q}{(2\pi)^2} \sum_{\text{all }\{n_i\}} \Bigg\{ \prod_i \frac{d^3k_i}{(2\pi)^3 2k_i^0} \int d^2b\, e^{-i(\vec{1}-\vec{q})\cdot\vec{b}} e^{-A(s,\vec{b})} \\
&\qquad \times \prod_j \left[\left(\frac{i}{2s}\right)\tilde{M}_j(s,\vec{b};\{k\})\right] \int d^2b'\, e^{-i\vec{q}\cdot\vec{b}'} e^{-A(s,\vec{b}')} \prod_j \left[\left(-\frac{i}{2s}\right)\tilde{M}_j(s,\vec{b}';\{k\})\right]\Bigg\} \\
&= -2s \int d^2b\, e^{-i\vec{1}\cdot\vec{b}} e^{-2A(s,\vec{b})} \sum_{\text{all }\{n_i\}} \int \left(\prod_i \frac{d^3k_i}{(2\pi)^3 2k_i^0}\right) \prod_{j=1}^{N} \left|\frac{1}{2s}\tilde{M}_j(s,\vec{b};\{k\})\right|^2,
\end{aligned} \tag{3.22}$$

where $\{n_i\}$ denotes the numbers of rungs in the open ladders. The last integrals in (3.22) have already been worked out in Eqs. (3.13)–(3.15). Equation (3.22) then becomes

$$[\text{r.h.s. of } (3.19)]_{N\text{ open ladders}} = -2s \int d^2b\, e^{-i\vec{1}\cdot\vec{b}} e^{-2A(s,\vec{b})} \frac{[2A(s,\vec{b})]^N}{N!}. \tag{3.23}$$

The total inelastic contribution can be obtained from (3.23) by summing over N, giving

$$\begin{aligned}
[\text{r.h.s. of } (3.19)]_{\text{inelastic}} &= -2s \int d^2b\, e^{-i\vec{1}\cdot\vec{b}} e^{-2A}(e^{2A}-1) \\
&= -2s \int d^2b\, e^{-i\vec{1}\cdot\vec{b}}(1-e^{-2A(s,\vec{b})}).
\end{aligned} \tag{3.24}$$

Adding together (3.21) and (3.24), we have

$$\text{r.h.s. of } (3.19) = -2s \int d^2b\, e^{-i\vec{1}\cdot\vec{b}}(2-2e^{-A(s,\vec{b})}). \tag{3.25}$$

The left-hand side of (3.19) can be computed directly from (2.13) as

$$\text{l.h.s. of } (3.19) = -2s \int d^2b\, e^{-i\vec{1}\cdot\vec{b}}(2-2e^{-A(s,\vec{b})}) = \text{r.h.s. of } (3.19).$$

Thus, the amplitude of our model indeed satisfies the nonforward s-channel unitarity.

Notice that in our model

$$T_{fi}^\dagger = T_{if}^* = T_{fi}^*,$$

so that the left-hand side of (3.19) is simply twice the imaginary part of the nonforward elastic amplitude (2.13).

IV. PREDICTIONS AND RESULTS

In this section, we present various predictions of our model in detail. We shall emphasize those results which we believe to be more general than the simple model suggests.

In Sec. II we have already discussed the high-energy properties of the integrated elastic cross section and of the total cross section for various coupling strengths. Let us now discuss the differential elastic cross section (2.16). In the case of critical coupling, we have

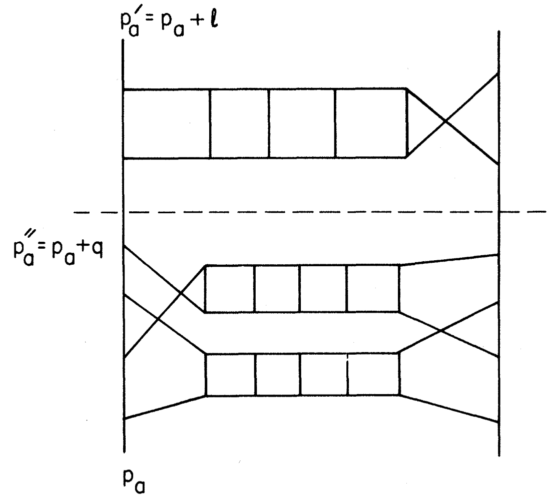

FIG. 7. Example of a contribution from the elastic channel to the nonforward unitarity sum.

$$\frac{d\sigma_E}{d\vec{k}^2} = \left(\frac{d\sigma_E}{d\vec{k}^2}\right)_0 \exp\left(-\frac{2}{3}\frac{\vec{k}^2}{\mu^2}\ln\frac{s}{\mu^2}\right), \tag{4.1}$$

where $(d\sigma_E/d\vec{k}^2)_0 = \pi/4\mu^4$ is the value of $d\sigma_E/d\vec{k}^2$ at $\vec{k}^2=0$. This differential cross section has an s-independent peak and a width decreasing logarithmically with s. For fixed s, the differential cross section drops off exponentially with momentum transfer squared.

In the case of strong coupling, the elastic amplitude is simply

$$\begin{aligned} T_E &= -2is\int d^2b\, e^{-i\vec{k}\cdot\vec{b}}\,\theta(b_m - b) \\ &= -i(4\pi b_m{}^2 s)\,\frac{J_1(b_m k)}{b_m k}, \end{aligned} \tag{4.2}$$

where b_m is given by (2.25), and $J_1(x)$ is the Bessel function of order 1. The differential cross section is

$$\frac{d\sigma_E}{d\vec{k}^2} = \pi b_m{}^4\left[\frac{J_1(b_m k)}{b_m k}\right]^2. \tag{4.3}$$

The height of the elastic peak grows like $(\ln s)^4$ since $b_m \sim \ln s$. The width of the elastic peak is determined by the first zero of $J_1(x)/x$, denoted as x_1, i.e.,

$$b_m{}^2 k_0{}^2 = x_1, \tag{4.4}$$

which implies that the product of $k_0{}^2$ corresponding to the first minimum of $d\sigma_E/dk^2$ and of the total cross section σ_T is a universal constant. Furthermore, the width of the elastic peak shrinks as $1/\ln^2 s$, and the integrated elastic cross section behaves like $(\ln s)^2$. Notice that (4.2)–(4.4) are general results of scattering by a circular black disk of radius b_m.

It is worth mentioning that a correlation generally exists between the shrinkage of the width of the elastic peak and the total cross section, if the latter increases with s. This follows simply from unitarity. The optical theorem states

$$\left(\frac{d\sigma_E}{d\vec{k}^2}\right)_0 = \frac{1}{4\pi}\left[\sigma_T{}^2(s) + \left|\frac{1}{s}\mathrm{Re}\,T_E\right|^2\right]. \tag{4.5}$$

Thus the height increases like $\sigma_T{}^2(s)$. On the other hand, we must have $\sigma_E < \sigma_T$; therefore the width must shrink at least as fast as $1/\sigma_T(s)$.

We now turn to the production processes and calculate first the one-particle spectrum. The one-particle spectrum is both useful and directly measurable. We can learn from it not only the momentum distribution, but the average multiplicity, inelasticity, etc., as well. To obtain the one-particle spectrum, we compute the cross section by integrating over the momenta of all final particles except one. This is equivalent to the experimental situation of putting a counter at a fixed angle and measuring the cross section and momentum distribution of an arbitrary final particle. We shall concentrate our attention only on the particles whose momenta satisfy the restriction (3.12) in the c.m. system. In this system the two high-energy final particles carry away practically all the large momenta of the incident particles. Experimentally, these particles move in the beam direction and can hardly be observed.

In a diagram with N open ladders, the differential cross section is given by (3.11). When a particle is detected, only the particular ladder in which the detected particle is associated with will be affected. The contributions due to the unopen ladders and the remaining open ladders are the same as in $\sigma^{(N)}$ [see Eq. (3.16)], and give a factor

$$e^{-2A(s,\vec{b})}\,\frac{1}{(N-1)!}\,[2A(s,\vec{b})]^{N-1},$$

where $1/(N-1)!$ instead of $1/N!$ appears since the detected particle may originate from any one of the N open ladders. After including the contributions due to all N, we find that this factor reduces to

$$e^{-2A(s,\vec{b})}\sum_{N=1}^{\infty}\frac{1}{(N-1)!}\,[2A(s,\vec{b})]^{N-1} = 1.$$

Thus, the contributions due to unopen ladders and the undetected open ladders cancel each other. We believe that the cancellation of the absorption correction and of the integrated production amplitude is a general feature of the theory, and is not restricted to the ladder diagrams used in our model. The one-particle spectrum obtained from our model is then identical to that obtained from the simple multiperipheral model such as shown in Fig. 5(b),

$$d\sigma_1=\left[\int d^2b\left(\prod_i{}' \frac{d^3k_i}{(2\pi)^3 2k_i^0}\right)\left|\frac{1}{2s}\tilde{M}(s,\vec{b};\{k_i\})\right|^2\right]\frac{d^3k}{(2\pi)^3 2k^0}$$

$$=\left[\int \frac{d^2l}{(2\pi)^2}\left(\prod_i{}' \frac{d^3k_i}{(2\pi)^3 2k_i^0}\right)\left|\frac{1}{2s}M(s,\vec{l};\{k_i\})\right|^2\right]\frac{d^3k}{(2\pi)^3 2k^0}, \tag{4.6}$$

where Π_i' stands for the product of all momentum integrals except for particle k.

Under the approximation of keeping only the leading $(\ln s)^N$ terms, we find that only the transverse integrations over the two adjacent loops are affected by fixing the observed particle momentum as k (see Fig. 8 with $\Delta=0$). The contribution due to these two adjacent loops is

$$g^2 f(\vec{k}^2)\,\frac{d^3k}{2(2\pi)^3k^0}$$
$$=\int \frac{d^2q}{(2\pi)^2}\,\frac{g^2}{(\vec{q}^2+\mu^2)^2}\,\frac{g^2}{[(\vec{q}+\vec{k})^2+\mu^2]^2}\,\frac{d^3k}{(2\pi)^3 2k^0}, \tag{4.7}$$

where k is the momentum of the detected particle. We have suppressed the dq_+dq_- integrals which will give a $\ln s$ factor as before. The contribution from the remaining loop integrals is

$$g^2[\alpha(0)+1]^{n-1}\frac{[\ln(s/\mu^2)]^{n-1}}{4s^2(n-1)!}, \tag{4.8}$$

where $1/(n-1)!$ instead of $1/n!$ appears for the reason that the detected particle can be any one of the n particles in the particular ladder. Combining (4.6) and (4.7) and summing over n, we have the one-particle spectrum

$$d\sigma_1=4\pi\beta(0)\left(\frac{s}{\mu^2}\right)^{\alpha(0)-1} f(\vec{k}^2)\,\frac{d^3k}{(2\pi)^3 2k^0}. \tag{4.9}$$

This one-particle spectrum has several interesting as well as some objectionable features. First, we find that the longitudinal-momentum distribution exhibits a dx/x distribution law as suggested by Feynman[2] and others,[1] and is supported by some recent experiments. Next, the transverse momentum reveals an s-independent distribution.

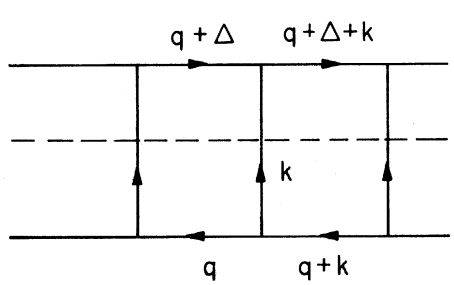

FIG. 8. Kinematics of the two adjacent loops affected by fixing the momentum vector k. The dashed line represents the unitarity cut.

This s-independent transverse-momentum distribution has been observed by both the accelerator and cosmic-ray experiments. However, the transverse-momentum spectrum predicted by (4.9) does not decrease fast enough to account for the observed fast falloff. Our model predicts a $1/k^4$ falloff, while all present available data indicate either a Gaussian or an exponential falloff for the transverse momentum. This slow falloff for the transverse momentum is due to the lack of long-chain correlation and the pointlike vertices in this model. Notice that in the case of weak and strong couplings the one-particle spectrum has an explicit s dependence. This s dependence disappears in the case of critical coupling and (4.9) has the scaling property proposed by Feynman.[2]

The average multiplicity is defined as

$$\langle n\rangle=\frac{\sum_n n\sigma_n}{\sigma_I}. \tag{4.10}$$

and is related to the one-particle spectrum by

$$\int d\sigma_1=\sum_n n\sigma_n=\sigma_I\langle n\rangle, \tag{4.11}$$

where σ_n is the partial cross section from final states with n particles identical to the one being detected. From (4.9) we obtain

$$\sigma_I\langle n\rangle=\int d\sigma_1=\frac{\pi g^2}{\mu^4}[\alpha(0)+1]^2\ln\left(\frac{s}{\mu^2}\right)\left(\frac{s}{\mu^2}\right)^{\alpha(0)-1} \tag{4.12}$$

Note that the two fast-moving particles are not included in (4.12). Thus, the total multiplicity should be $\langle n\rangle+2$. The $\langle n\rangle$ may be viewed as the number of additional particles emitted. For weak and critical couplings $[\alpha(0)\le 1]$, we obtain

$$\langle n\rangle=[\alpha(0)+1]\ln\left(\frac{s}{\mu^2}\right)=g^2\ln\left(\frac{s}{\mu^2}\right)\Big/16\pi^2\mu^2. \tag{4.13}$$

For strong coupling $[\alpha(0)>1]$, however, the multiplicity is

$$\langle n\rangle=\frac{\text{const}}{\ln(s/\mu^2)}\left(\frac{s}{\mu^2}\right)^{\alpha(0)-1}. \tag{4.14}$$

Expression (4.14) has a serious defect. As the coupling becomes very strong, the multiplicity predicted by (4.14) may increase faster than $\sqrt{s}/\mu$. This is certainly unacceptable because the total energy carried by the inelastic states is larger than the $\sqrt{s}$ allowed by energy conservation. The inconsistency in the present case can be traced back to the inadequacy of our approximation, which neglects the energies of the soft particles in the energy-conservation condition and ignores the contribution from nonleading $(\ln s)^N$ terms. The $(\ln s)^N$ factors, which eventually exponentiate to a power of s, come from the longitudinal phase-space integrals

$$2\int_0^{\sqrt{s}} \frac{dk^3}{k^0} = 2\int_\mu^{\sqrt{s}} \frac{dk_+}{k_+} = \ln\left(\frac{s}{\mu^2}\right). \tag{4.15}$$

The upper limit is only an order-of-magnitude estimate. A more reasonable cutoff is to assume that the upper limit is most probably given by the average energy shared by each particle, $s/\langle n\rangle$. If $\langle n\rangle$ grows as a power of s, as in the strong-coupling case, the correction becomes significant. To correct this error, we propose a self-consistent physical procedure. Let us assume that, within an insignificant logarithmic correction,

$$\langle n\rangle \propto (s/\mu^2)^a, \tag{4.16}$$

where a is a parameter to be determined. This procedure will affect our previous results by the substitution

$$\ln(s/\mu^2) \to (1-2a)\ln(s/\mu^2) \tag{4.17}$$

in the elastic and inelastic amplitudes. The same cutoff is to be applied to every particle, virtual or real, so that general principles such as unitarity can be maintained. Equation (4.14) is modified to

$$\begin{aligned}\langle n\rangle_c &= \frac{\text{const}}{\ln(s/\mu^2)}\left(\frac{s}{\mu^2}\right)^{\alpha(0)(1-2a)-(1+2a)}\\ &= \frac{\text{const}}{\ln(s/\mu^2)}\left(\frac{s}{\mu^2}\right)^{a},\end{aligned} \tag{4.18}$$

as we demand that this expression be consistent with the original assumption (4.16). This gives

$$a = \frac{(g^2/16\pi^2\mu^2)-2}{(g^2/8\pi^2\mu^2)+1} = \frac{\alpha(0)-1}{2\alpha(0)+3} = \overline{\alpha}(0)-1. \tag{4.19}$$

As $g^2\to\infty$, a approaches the limit $\frac{1}{2}$, no longer in conflict with energy conservation. Thus, the only modification is to replace $\alpha(\vec{k}^2)+1$ in the strong-coupling case by $\overline{\alpha}(\vec{k}^2)+1=(1-2a)\times[\alpha(\vec{k}^2)+1]$, in the amplitude as well as in other final expressions. Let us understand that this is done wherever it is applicable. Again, we are only interested in the general features of the model, and none of these features is affected by the modification.

Our proposed cutoff procedure, which makes the average multiplicity consistent with energy conservation, can only be regarded as temporary. A more satisfactory solution is certainly needed. However, even in this crude treatment, our procedure has the interesting consequence that the total cross section cannot grow indefinitely with increasing coupling constant. It approaches a limit:

$$\sigma_T \xrightarrow[g^2\to\infty]{} \frac{5}{3}\frac{\pi}{\mu^2}\ln^2 s.$$

The multiplicity difficulty encountered in this study is a warning of the danger hidden in this approach of summing leading terms. This is particularly so as the inconsistency cannot be easily detected in the gross results such as the elastic amplitude and the elastic and total cross sections.

For a many-particle spectrum and for a number distribution, the situation is rather subtle. For example, there are two competing mechanisms which contribute to the two-particle spectrum. Namely, either these two detected particles are from the same open ladder, or they are from two different open ladders. The contribution due to the first mechanism, for the same reason as in obtaining the one-particle spectrum, leads to a two-particle spectrum which is the same as those derived from the multiperipheral process. In particular, it has a simple s-dependence factor $s^{\alpha(0)-1}$, just as in the one-particle case. However, the contribution due to the second mechanism leads to two independent one-particle emissions in the impact-parameter space. Hence, in the impact-parameter space, the two-particle spectrum is simply a product of two independent one-particle spectra. It has an s-dependence factor $s^{2[\alpha(0)-1]}$, which is the product of two s-dependence factors for individual one-particle spectra. Thus, the first mechanism dominates over the second if $\alpha(0)-1<0$, and vice versa if $\alpha(0)-1>0$. Hence we find that for weak coupling, the first mechanism always dominates, and the multiparticle spectrum is given by the same amplitude as in the multiperipheral model. For strong coupling, on the other hand, the second mechanism dominates and the multiparticle spectrum in the impact space is predominantly the product of individual one-particle spectra. For critical coupling, the two mechanisms are comparable. A careful study reveals that the first mechanism still dominates through factors of $\ln s$. The above results are general, and are *not* confined to ladder diagrams. A simple consequence of the above results is that we should expect some correlation in the multiparticle spectrum at high energy for weak and critical couplings,[17] and should see none in the strong-coupling case. The multiparticle correlation effects should be looked for experimentally.

Once we know that the multiparticle spectrum is dominated by the multiperipheral amplitude in the weak and the critical coupling, we can compute the multiparticle distribution function easily. The distribution laws for the multiperipheral process are well known. Readers are referred to the original literature for details. In particular, the number distribution due to leading terms is a Poisson distribution.[18] Thus, the number distribution in our model for weak and for critical coupling is likewise a Poisson distribution,

$$P(n)=\frac{1}{n!}[\alpha(0)+1]^n\left(\ln\frac{s}{\mu^2}\right)^n\left(\frac{s}{\mu^2}\right)^{-\alpha(0)-1}. \quad (4.20)$$

The average multiplicity is $\langle n\rangle=[\alpha(0)+1]\ln(s/\mu^2)$, as obtained in (4.13).

For strong coupling, the spectrum for N particles detected is the product of individual one-particle spectra in impact-parameter representation,

$$d\sigma_N=\int d^2b\prod_{i=1}^{N}\left[B(s,\vec{b};\vec{k}_i)\frac{d^3k_i}{(2\pi)^3 2k_i^0}\right], \quad (4.21)$$

where

$$B(s,\vec{b};\vec{k})=\sum_n\int\prod'_{n-1\text{ undetected rungs}}\left(\frac{d^3k_a}{(2\pi)^3 2k_a^0}\right)\left|\frac{1}{2s}\tilde{M}(s,\vec{b},k_a)\right|^2, \quad (4.22)$$

with $\tilde{M}(s,\vec{b},k_a)$ being given in (3.3) and (3.5). In analogy to (4.9), a typical one-particle contribution from a single open ladder reduces to

$$\begin{aligned}B(s,\vec{b};\vec{k})&=\int\frac{d^2\Delta}{(2\pi)^2}e^{i\vec{\Delta}\cdot\vec{b}}\left\{\sum_n\int\frac{d^2l}{(2\pi)^2}\prod'_{n-1\text{ undetected rungs}}\left(\frac{d^3k_a}{(2\pi)^3 2k_a^0}\right)\left[\frac{1}{2s}M(s,\vec{l};k_a)\right]\left[\frac{1}{2s}M(s,\vec{l}+\vec{\Delta},k_a)\right]^*\right\}\\&=\int\frac{d^2\Delta}{(2\pi)^2}e^{i\vec{\Delta}\cdot\vec{b}}\frac{g^4}{4\mu^4}\left(\frac{s}{\mu^2}\right)^{\alpha(\vec{\Delta}^2)-1}f(\vec{\Delta},\vec{k})\\&\approx\frac{\beta(0)(s/\mu^2)^{\alpha(0)-1}}{c\ln(s/\mu^2)}e^{-\vec{b}^2/4c\ln(s/\mu^2)}f(\vec{k}^2),\end{aligned} \quad (4.23)$$

with

$$f(\vec{\Delta},\vec{k})=g^2\int\frac{d^2q}{(2\pi)^2}\frac{1}{(\vec{q}^2+\mu^2)[(\vec{q}+\vec{\Delta})^2+\mu^2]}\frac{1}{[(\vec{q}+\vec{k})^2+\mu^2][(\vec{q}+\vec{k}+\vec{\Delta})^2+\mu^2]}, \quad (4.24)$$

$$f(0,\vec{k})=f(\vec{k}^2), \quad (4.25)$$

and c is given in (2.23).

The number distribution for strong coupling can be obtained easily from the multiparticle distribution (4.21). Since the individual emission is an independent event in the impact-parameter space, one expects a simple Poisson distribution in the impact-parameter representation,

$$P(N)=\frac{1}{\sigma_I}\int d^2b\,e^{-B(s,\vec{b})}[B(s,\vec{b})]^N/N!. \quad (4.26)$$

$B(s,\vec{b})$ is obtained by integrating over the one-particle spectrum function:

$$\begin{aligned}B(s,\vec{b})&=\int\frac{d^3k}{(2\pi)^3 2k^0}B(s,\vec{b},\vec{k})\\&=\frac{\pi g^2}{\mu^2}\int\frac{d^2\Delta}{(2\pi)^2}e^{i\vec{\Delta}\cdot\vec{b}}[\alpha(\vec{\Delta}^2)+1]^2\\&\quad\times\left(\frac{s}{\mu^2}\right)^{\alpha(\vec{\Delta}^2)-1}\ln\frac{s}{\mu^2}\\&=\text{const}(s/\mu^2)^{\alpha(0)-1}e^{-b^2/4c\ln(s/\mu^2)}.\end{aligned} \quad (4.27)$$

Note that $B(s,\vec{b})$ is related simply to the opaqueness $A(s,\vec{b})$, and has the same size b_m. The last relation implies that

$$\begin{aligned}\sum_{N=1}^{\infty}P_N&=\frac{1}{\sigma_I}\int d^2b\,e^{-B(s,\vec{b})}(e^{B(s,\vec{b})}-1)\\&=\frac{1}{\sigma_I}\int d^2b(1-e^{-B(s,\vec{b})})\\&\approx\pi b_m^2/\sigma_I=1,\end{aligned} \quad (4.28)$$

as required. Equation (4.26) has a longer tail at large N than a single Poisson distribution.

As a check of (4.26), we compute various moments of the number distribution from both (4.21) and (4.26). The moments of the number distribution from (4.21) give

$$\int d\sigma_M = \sum_N \sigma_N C_M^N = \sigma_I \sum_N \frac{\sigma_N}{\sigma_I} C_M^N = \sigma_I \langle C_M^N \rangle$$

$$= \frac{1}{M\,!} \int d^2 b \left[\int \frac{d^3 k}{(2\pi)^3 2k^0} B(s, \vec{b}, \vec{k}) \right]^M$$

$$= \frac{1}{M\,!} \int d^2 b [B(s, \vec{b})]^M, \qquad (4.29)$$

where $C_M^N = N!/M\,!(N-M)\,!$ represents the number of ways that M particles can be selected from a final state with N particles identical to the ones observed, and $1/M\,!$ is a statistical factor associated with M identical particles. Equation (4.29) implies

$$\sigma_I \langle N(N-1)\cdots(N-M+1)\rangle = \int d^2 b [B(s, \vec{b})]^M. \qquad (4.30)$$

This is precisely the moment of the number distribution predicted from the Poisson distribution (4.26). Thus, Eq. (4.26) reproduces *all* moments of the number distribution, and is indeed the correct distribution.

V. DISCUSSION

Even though our result is based on the sum of leading $(\ln s)^N$ terms in t-channel ladders, it can be generalized to include nonleading $(\ln s)^N$ terms or other types of exchange as well.

Before we sketch how the generalization can be actually carried out, we like to emphasize that grouping together terms in the perturbation series with same powers of the coupling constant and same high-energy behavior is not the most effective approach to reveal the general features of the problem. That is because various terms of this nature may correspond to different physical mechanisms. If one wishes to study the general features of a specific mechanism, obviously one should sum only those terms which correspond to this mechanism, and should not group those terms with others strictly according to the conventional perturbation prescription.

For example, we recall that the leading term in a t-channel ladder with $(n+2)$ rungs behaves like $s^{-1}(\ln s)^N$, and this contribution comes from the kinematic region where the momenta p_+'s of the n inelastically produced particles satisfy the restriction (2.7). In other words, the p_+ of a particle in the chain is much smaller than that of the particle before it and much larger than that of the one after it. Let us call "the projectile" the particle with large p_+ in the c.m. system, and "the target" the particle with large p_- in the c.m. system. If we now allow the large p_+ (p_-) to be shared by two or more particles, these particles will have s-independent finite momenta in the rest frame of the projectile (target). Inclusion of these additional kinematic regions will produce certain nonleading terms to the t-channel ladder amplitude. There is another mechanism to produce nonleading terms: to allow several particles next to each other in the middle of the chain to have comparable p_+'s. These two types of nonleading terms, are, however, associated with totally different physical situations. Therefore, they should be treated separately. The first type is associated with the fragmentation processes, and the second type with the correlation of the pionization products. [We adopt the definition that particles which carry finite momenta in the rest frame of the target (projectile) are the fragments of the target (projectile). The upper limit of these momenta may be chosen to be rather large or rather small; nevertheless, it is s-independent. We call all remaining particles pionization products. These pionization particles carry a typical energy s^a, $0<a<1$, at large s in the rest frame of the target or the projectile.]

In the present paper we concentrate our attention on the pionization processes. Any possible fragmentation events are totally neglected. What we like, to generalize the results obtained in the previous sections, is to introduce correlations among the pionization particles, and to include other kinds of connected pieces beyond the simple t-channel ladders. Therefore, we will still make the assumption that the incident particles retain their large momenta during the scattering, so that only pionization particles are produced. This assumption is sufficient to obtain the eikonal form for the elastic amplitude. As shown in Ref. 8, the s-channel iteration of an arbitrary connected piece, either leading or nonleading, leads automatically to an eikonal form,

$$-2is \int d^2 b\, e^{-i\vec{k}\cdot\vec{b}}(1 - e^{-A(s,\vec{b})}), \qquad (5.1)$$

where $iA(s, \vec{b})$ is a (complex) potential due to the particular connected unit. When more than one kind of connected pieces are iterated, $A(s, \vec{b})$ is the sum of the contributions from each connected unit.

The total elastic, total inelastic, and total cross sections for processes involving the iteration of one or more arbitrary connected pieces are found to be

$$\sigma_E = \int d^2 b (1 - e^{-A(s,\vec{b})})(1 - e^{-A(s,\vec{b})})^*, \qquad (5.2)$$

$$\sigma_I = \int d^2 b (1 - e^{-A(s,\vec{b}) - A(s,\vec{b})^*}), \qquad (5.3)$$

and

$$\sigma_T = \int d^2b(2 - e^{-A(s,\vec{b})} - e^{-A(s,\vec{b})^*}) = \sigma_E + \sigma_I, \tag{5.4}$$

respectively, where the over-all potential $iA(s, \vec{b})$ is obtained from the sum of *all* possible connected diagrams. The high-energy behavior of the cross sections, and the general distribution properties discussed in the previous sections, remain qualitatively valid if we define the weak, critical, and strong coupling according as

$$\mathrm{Re}\tilde{A}(s, t=0) < s, \ \sim s, \ \text{or} > s, \tag{5.5}$$

at large s. At the present time we are not able to say much about this over-all $A(s, \vec{b})$, except that it has a positive real part for all $\vec{b}$. A positive $\mathrm{Re}A(s, \vec{b})$ implies an absorptive potential, and is necessary to insure the amplitudes to satisfy s-channel unitarity. It is hoped that the power dependence of s in the over-all potential iA might approach a limiting value at the strong-coupling limit, as a too rapid increase of the potential leads to a too rapid increase of the final-particle multiplicity. In other words, the difficulty encountered in Sec. IV may cure itself in a more complete theory, without our having to impose the energy-conservation condition explicitly. To a lesser degree, we have studied the effect of other connected pieces by including also the nonleading $(\ln s)^N$ terms in a ladder diagram. A preliminary investigation indicates that the correction due to these nonleading $(\ln s)^N$ terms is indeed in the right direction, and the resultant s dependence in the full ladder amplitude increases much slower than that in the original ladder amplitude. The result of this investigation will be published in the future.

Our model may be viewed as a field-theoretical justification of the conventional absorption model. In particular, our calculation leads to a generalization of the absorption model to the production processes. One can see from this model that it is the virtual pionization processes which are responsible for the s dependence in the absorptive potential. The production and absorption mechanisms are closely related. It is the self-consistency of the model and the intrinsic relation between the absorptive correction and the production processes that we would like to emphasize here.

Our model has also important implications on the recently proposed model(s)[19] based on the unitarity correction to the simple Regge amplitude, by using the simple Regge amplitude as a potential in an eikonal form. If one accepts that a Regge amplitude is generated from the sum of a set of t-channel connected exchanges, such as in the ladder diagrams, we find that the eikonalization of the Regge amplitude emerges naturally after s-channel iteration. In particular, the same mechanism which generates the Regge amplitude as a potential is also responsible for the production of the final inelastic states.

As mentioned before, we have not taken any fragmentation process into account. Obviously, many of our results will be modified, if the large momentum of an incident particle is shared by two or more particles. These particles will be realized as fragments in the final states. Those results that are based on a single impact parameter are very likely to be modified. However, the distribution properties of the final states in the region of small p_+'s in the c.m. system and the s dependence of the cross sections, which are dominated by the pionization products, will probably not be affected. This is based on the observation that a typical pionization particle travels with a momentum which is vastly different from those of the incident particles, and is produced in general through a cascade of real or virtual processes. Hence, the dependence of the distribution properties of these pionization particles on the incident particles is very likely to be washed out, and we end up with some universal distribution. This is particularly true for the cases of weak coupling and critical coupling in which the particles are emitted from a long chain.

In a more general, though not necessarily perfect, approach, we may picture that both the colliding particles first dissociate into fragments, and that the fragments from the target scatter with those from the projectile. Our present calculation presumably applies only to the individual scattering between the fragments.

Perhaps a remark on some related calculations in QED is in order. It is known that the general eikonal form holds also for $e^-e^{\mp}$ scatterings in QED after the s-channel iteration of an arbitrary connected t-channel exchange. We expect that many of our results generalize to QED. Recently, the s-channel iteration of tower diagrams was carried out and led to results similar to those of the absorption model. Nevertheless, there is a fundamental difference between QED and the φ^3 theory. The basic interaction in QED is vector in nature, and the potential is proportional to s, to start with. The high-order interactions seem to increase the power dependence of s in the effective potential, and thus lead automatically to a strong-coupling theory for any nonvanishing coupling. Indeed, the results obtained in QED calculations are analogous to our results for the strong-coupling case. However, according to our calculations, the strong-coupling case is only one of the possible alternatives. At the present time, one cannot tell which one of the alternatives is the best description of the real world. Further experiments on total cross sections, multiplicities, and multiparticle spectra should differentiate between them.

To conclude, we remind ourselves, and the readers, of two central questions remaining unanswered in this diagram-analysis approach.

(1) There are infinitely many classes of diagrams in any field-theory model. Yet we are able to study only very limited classes of these, and only in certain kinematic regions. We would like to know whether the qualitative properties inferred from such a limited study as ours will persist when other classes of diagrams are included. A point of special interest lies in the question: What is the effect of enforcing the full crossing symmetry, not just the *su* crossing symmetry?

(2) So far, field-theoretic studies have to rely on perturbation expansions. The usual procedure is to first take the high-energy limit of each term, and then resum again to obtain the result. Although this exchange of limit is known not to affect the qualitative feature of the true limit of the sum for the simple multiperipheral amplitude, is that also true for more general amplitudes?

Added note. Since this work was finished we have received preprints on related subjects by various authors.[20] These papers are concerned with the validity of the simple eikonal representation for the elastic amplitude arising from the s-channel interaction of t-channel ladders, or the overcounting problem peculiar to a φ^3 theory.

As we have already emphasized and indicated in the text, the simple eikonal form for the elastic amplitude emerges only if it is assumed that in the c.m. system the two incident particles retain their large momenta in the scattering process. This assumption is equivalent to the neglect of all fragmentation events. We also suggested that the pionization and fragmentation processes (as defined in the text) should be treated separately. The simple eikonal representation no longer holds once the fragmentation events are included. In the example of two-Reggeon exchange considered by Muzinich, Tiktopoulos, and Treiman, both pionization and fragmentation events are treated simultaneously. In this example of two-Reggeon exchange the fragmentation contributions introduce only an s-independent multiplicative factor. Therefore it is not suprising that although the coefficient differs from the simple eikonal picture, the power dependence on s is the same. Tiktopoulos and Treiman show that if one includes all the permutations of the legs of the exchanged ladders attached to the two incident-particle lines, many of the resultant diagrams are topologically equivalent, since the exchanged lines and the incident-particle lines are identical in φ^3 theory. Moreover, some of these diagrams possess totally different asymptotic high-energy behavior from what one expects if eikonalization is to work. The latter high-energy behavior comes about as a result of the fact that the large incident momenta can flow along more than one path in these diagrams.

Overcounting has never been a difficulty in our study because of the assumption that the two incident particles retain their large momenta during the scattering. Consequently, all the diagrams with attached legs permutated in all possible ways are different from one another via the distinct momentum values assigned to the various lines. This will cease to be true when the large incident momenta are allowed to be shared by several particles. In such a case these particles can no longer be distinguished by their momentum values and may therefore become identical. Thus, this complication of overcounting, as discussed by Tiktopoulos and Treiman, will arise when our consideration is extended to include fragmentation.

The question of overcounting is studied in some detail by Cicuta and Sugar, who reach essentially the same conclusion as ours. They explicitly show that each of the "overcounted diagrams" corresponds to each possible path for large-momentum flow in a single Feynman diagram. They also show that the diagrams with unusual high-energy behavior discussed by Tiktopoulos and Treiman actually correspond to exchanges of objects more complicated than the simple ladders between the two energetic lines. In addition, Cicuta and Sugar are able to show that the contributions from multiladder exchange summing to an eikonal form are those which give the leading contribution to the N-Reggeon cut in the weak-coupling limit.

Note added in proof. In their recent papers, Cheng and Wu[21] criticized in general the validity of the eikonal approximation in φ^3 perturbation calculation and emphasized the distinction between the φ^3 and the QED calculations. In particular, they referred explicitly to our work (Ref. 12). Thus, we would like to make a few remarks here:

(1) The validity of the eikonal approximation is guaranteed in our calculation as was explained in this paper and in Refs. 8 and 12. As we have pointed out, the eikonal approximation fails if one takes more complicated fragmentation processes into account. As far as the failure of the eikonal approximation is concerned, however, there is *no* fundamental physical difference between the φ^3 and the QED calculations. In both cases, the fragmentation regions will sum up to the same s-power dependence as the leading terms do. These higher-order fragmentation terms violate the simple

eikonal picture.

(2) Inclusion of the fragmentation processes will probably modify the full amplitude into an operator eikonal form, as suggested by the operator droplet model.[22] This possibility was remarked upon in Ref. 12 and is also discussed in the main text of the present paper. In contradiction to that claimed by Cheng and Wu,[23] the operator-droplet-model calculation reproduces the correct leading QED scattering amplitude, including the $(\ln s)^N$ terms.[24]

(3) As we have explained in the Discussion, we expect that the s dependence of the total cross sections and the distribution properties of the final particles in the pionization region are independent of the approximation used in the fragmentation regions. These properties have a simple analogy in the properties of a real gas. (See Refs. 2 and 25 for the analogies of the high-energy scattering and a real gas.) Namely, the distribution properties in the interior of a gas (which is analogous to the pionization region) and its pressure [which is analogous to the trajectory function $\alpha(t)$ in the s dependence of the amplitude] depend only on the density and the temperature of a gas, independent of the shape and the composition of the wall (which is analogous to the fragmentation region).

ACKNOWLEDGMENTS

The authors are indebted to Professor R. Blankenbecler, Professor L. Brown, Professor J. M. Cornwall, Professor S. Drell, and members of the Stanford Linear Accelerator Center for many stimulating discussions. They wish to thank Professor Sidney Drell for his hospitality at the Stanford Linear Accelerator Center where this work was started.

---

*Work supported in part by the National Science Foundation under Grant No. NSF GP19433.

†Work supported in part by the National Science Foundation.

[1]D. Amati, A. Stanghellini, and S. Fubini, Nuovo Cimento 26, 896 (1962). See also K. Wilson, Acta Phys. Austriaca 17, 37 (1963).

[2]R. P. Feynman, Phys. Rev. Letters 23, 1415 (1969), and in *High Energy Collisions*, edited by C. N. Yang *et al.* (Gordon and Breach, New York, 1969).

[3]J. Benecke, T. T. Chou, C. N. Yang, and E. Yen, Phys. Rev. 188, 2159 (1969).

[4]For a conventional approach, see, e.g., R. J. Eden *et al.*, *The Analytic S-Matrix* (Cambridge Univ. Press, Cambridge, England, 1966).

[5]S. Weinberg, Phys. Rev. 150, 1313 (1966).

[6]H. Cheng and T. T. Wu, Phys. Rev. Letters 24, 1456 (1970), and references cited therein.

[7]S. J. Chang and S. Ma, Phys. Rev. 180, 1506 (1969); 188, 2385 (1969).

[8]S. J. Chang and P. M. Fishbane, Phys. Rev. D 2, 1104 (1970); 3, 1047 (1971).

[9]M. Lévy and J. Sucher, Phys. Rev. 186, 1656 (1969); R. L. Sugar and R. Blankenbecler, *ibid.* 183, 1387 (1969).

[10]For applications to leptonic processes, see S. D. Drell, D. J. Levy, and T. M. Yan, Phys. Rev. Letters 22, 774 (1969); Phys. Rev. 187, 2159 (1969).

[11]B. W. Lee and R. F. Sawyer, Phys. Rev. 127, 2266 (1962), and Ref. 4.

[12]S. J. Chang and T. M. Yan, Phys. Rev. Letters 25, 1586 (1970).

[13]B. Hasslacher, D. K. Sinclair, G. M. Cicuta, and R. L. Sugar, Phys. Rev. Letters 25, 1591 (1970).

[14]M. Froissart, Phys. Rev. 123, 1053 (1961).

[15]G. V. Frolov, V. N. Gribov, and L. N. Lipatov, Phys. Letters 31B, 34 (1970).

[16]The technique we describe here is slightly different from that developed in Ref. 8. The procedure given here can be generalized to calculate the nonleading powers of $\ln s$. A major new feature of the nonleading-term calculation is that one must also include contributions from negative values of the p_+'s. The details will appear in a future paper by the authors and Y. P. Yao.

[17]Kinematics restricts these correlations to groups of particles with small subenergies. Thus, there will be significant correlation only among particles emitted next to each other in the multiperipheral chain. In our approximation of keeping the leading $(\ln s)^N$ contributions, only transverse-momentum correlation exists. However, if nonleading $(\ln s)^N$ terms are included, longitudinal correlation will also be present.

[18]This Poisson distribution reflects the lack of longitudinal correlations in the leading $(\ln s)^N$ contributions. However, if nonleading $(\ln s)^N$ terms are included, the final particles will be correlated. Then the number distribution will no longer be Poisson.

[19]See, e.g., R. Arnold, Phys. Rev. 153, 1523 (1967); S. Frautschi and B. Margolis, Nuovo Cimento 56A, 1155 (1969).

[20]I. J. Muzinich, G. Tiktopoulos, and S. B. Treiman, Phys. Rev. D 3, 1041 (1971); G. Tiktopoulos and S. B. Treiman, *ibid.* 3, 1037 (1971); G. M. Cicuta and R. L. Sugar, *ibid.* 3, 970 (1971); B. Hasslacher and D. K. Sinclair, *ibid.* 3, 1770 (1971); H. Fried, *ibid.* 3, 2010 (1971).

[21]H. Cheng and T. T. Wu, Phys. Letters 34B, 647 (1971).

[22]T. T. Chou and C. N. Yang, Phys. Rev. 170, 1591 (1968); 175, 1832 (1968); B. Lee, Phys. Rev. D 1, 2361 (1970).

[23]H. Cheng and T. T. Wu, Phys. Rev. D 1, 2775 (1970).

[24]S. J. Chang, Phys. Rev. D 2, 2886 (1970).

[25]K. Wilson, Cornell University report, 1970 (unpublished).